EvNS-2017

Nuclear Compton scattering and Nuclear Magnetic Resonance, a common way to understand the local order

Francesco Mallamace

Carmelo Corsaro (Messina), Sow-Hsin Chen (MIT), Domenico Mallamace (CSGI Florence), Eugene H. Stanley (Boston), Cirino Vasi (CNR-IPCF), Ben Widom (Cornell).

Now

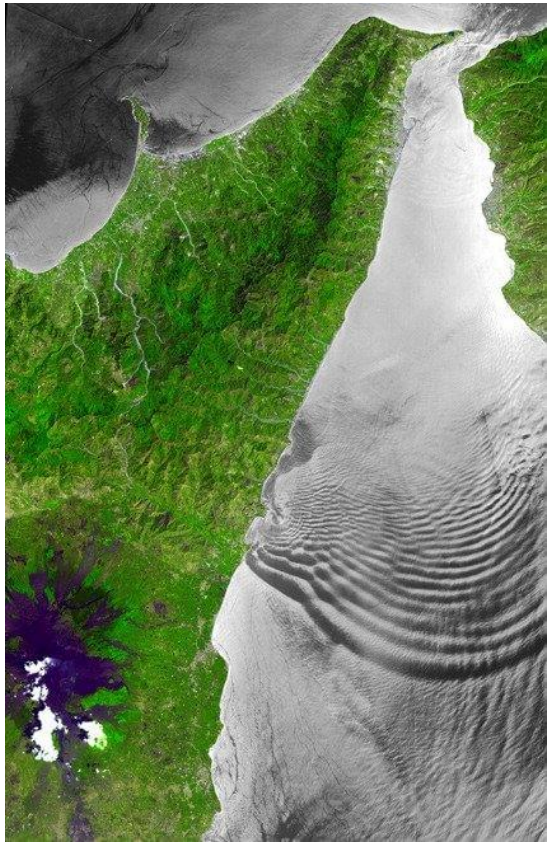

The future

Water

Hydrophobic Effect: hydrophilic and hydrophobic interactions.

The bulk water expansivity: its behavior evidences a special temperature (T_I)

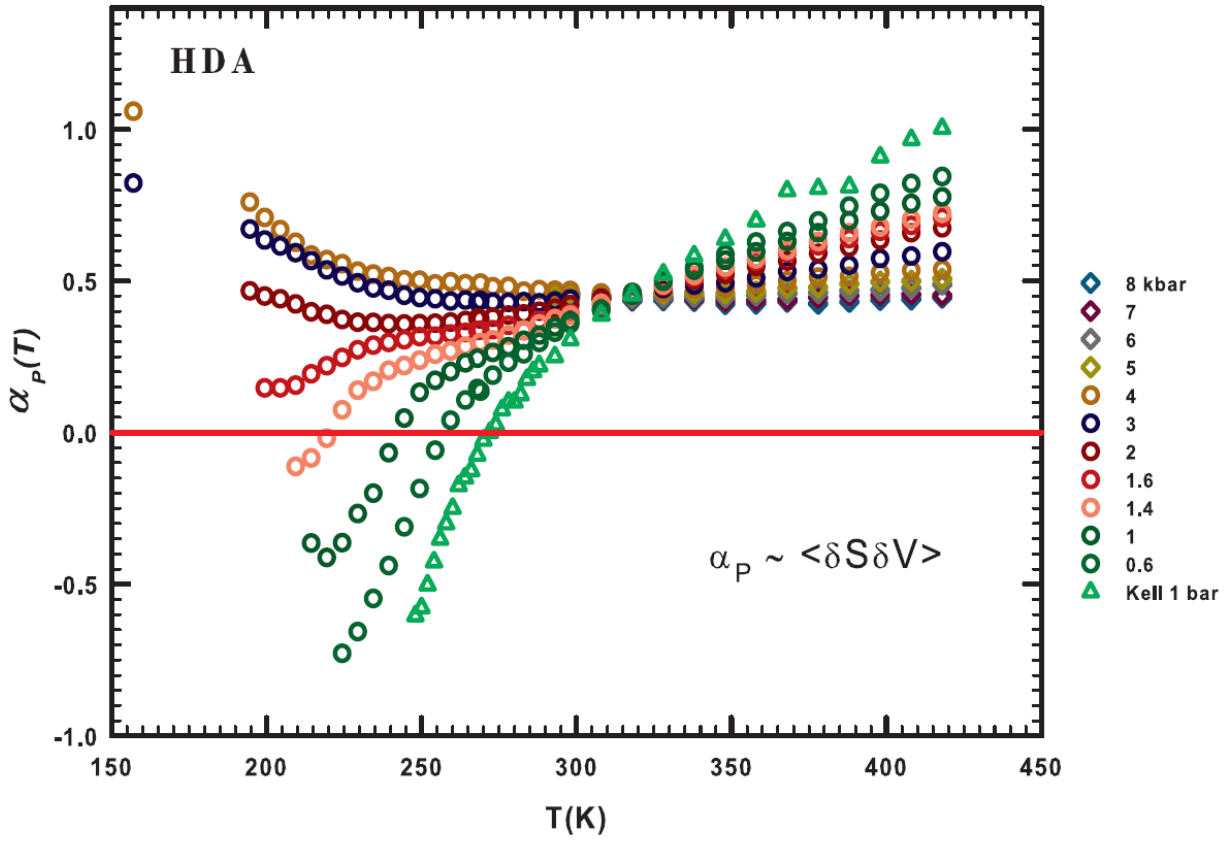

All curves at a given pressure cross at T_I

The onset of the water tetrahedral network at T*~315 K, was proposed by this and transport data, but never observed in an experiment focused on the system structure.

- ***T^*~315 K is a singular thermodynamically consistent temperature at the origin of the anomalous behavior of liquid water and supports the idea of a two liquid states for water.***
- ***By considering old and new data of both the isothermal compressibility $K_T(T,P)$ and the coefficient of thermal expansion $\alpha_P(T,P)$, it has been observed that K_T shows a minimum at T^*= 315±5K for all the studied pressures.***
- ***At the same temperature also the α_P behavior appears to be surprising, in fact all the corresponding curves (in the P−T plane) measured at different P cross at T^*. In other word these data show a "Universal Expansivity Point" at T^* and $\alpha_P(T^*)= 0.44\cdot10^{-3}\ K^{-1}$.***
- ***Unlike other water singularities, this temperature is consistent in the relationship connecting these two important thermodynamical response functions.***

$$\left(\frac{\partial \alpha_P}{\partial P}\right)_T = -\left(\frac{\partial \chi_T}{\partial T}\right)_P$$

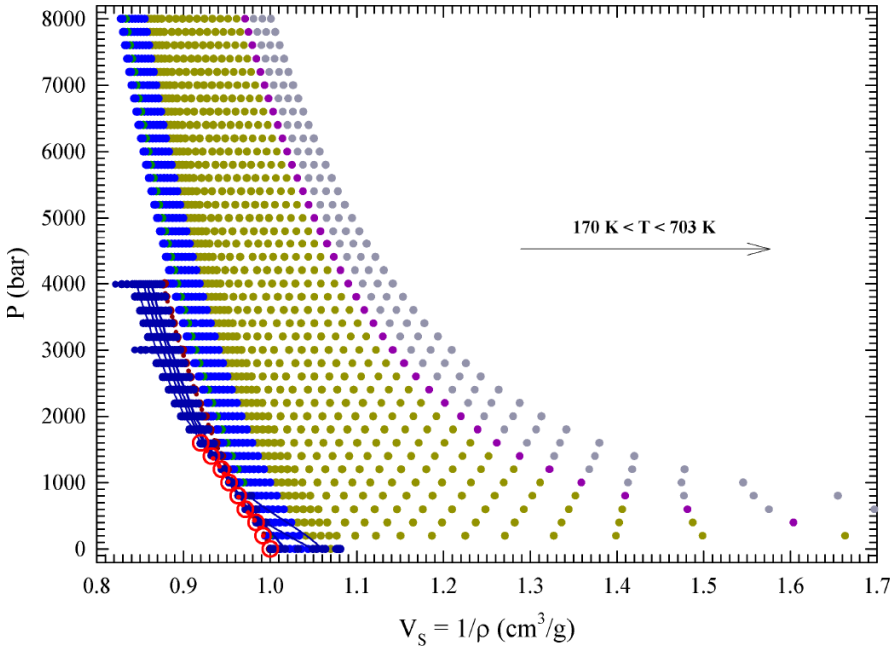

WATER – the Hydrogen bond effect in its liquid state.
The PV phase.

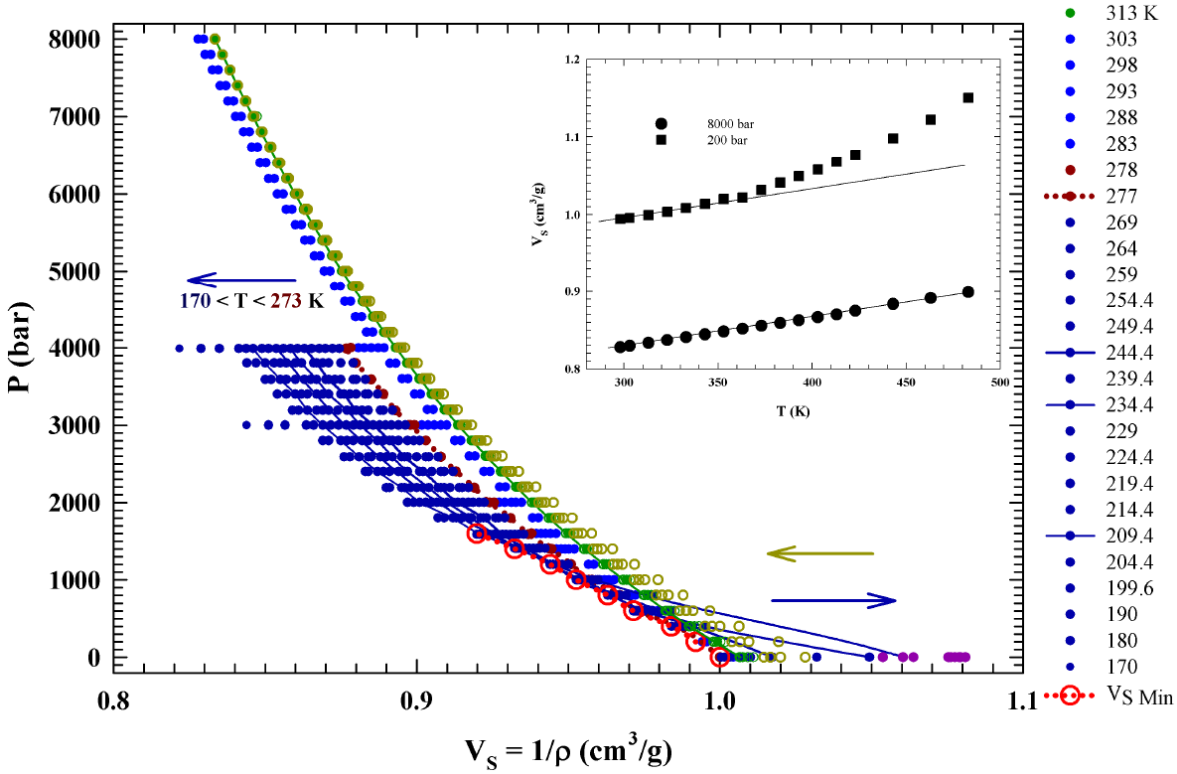

EvNS-2017

Nuclear Magnetic Resonance (NMR)

In NMR experiments the chemical shifts $\hat{\delta}$ is measured (as the change of resonance frequency of a nucleus) rather than the magnetic shielding tensor $\hat{\sigma}^{NMR}$

$$\hat{\delta} = 1\sigma_{iso}^{NMR} - \hat{\sigma}^{NMR} \qquad (1)$$

where 1 is the unit matrix and σ_{iso}^{NMR} is the isotropic value or trace $\sigma_{iso}^{NMR} \equiv Tr(\hat{\sigma}^{NMR}/3)$ of the shielding tensor of the standard reference used in the NMR experiments

In the liquid case the situation is different and may be of interest also the shielding anisotropy. A practical way to measure σ_{iso}^{NMR} is made via the measured proton chemical shift relative to a given standard through the relation

$$\delta = \sigma_{iso}^{NMR,ref} - \sigma_{iso}^{NMR} + (A - \frac{1}{3})(\chi^{ref} - \chi) \qquad (2)$$

χ is the magnetic susceptibility and the factor A depends on the sample shape and orientation; A = 1/3 for a spherical sample.

- The chemical shift is an assumed linear response of the electronic structure of a system under to a magnetic field B_0, as $B(j) = (1 - \beta_j)B_0$, where j is an index identifying the chemical environment.

- Both $\hat{\delta}$ and thus $\hat{\sigma}^{NMR}$ can be measured by the free induction decay (FID) containing information of all nuclear species in the studied sample whose resonance frequencies are in the harmonic content of the NMR radio frequency (RF) pulse.

- The $\hat{\sigma}^{NMR}$ sensitivity to the local environment makes it a powerful probe of hydrogen bonding, able to probe in a direct way the hydrogen bond structure (not only for ice).

- For liquid water proton $\hat{\sigma}^{NMR}$ is very nearly axially symmetric in the stable liquid phase and near its critical point, so that it given by the isotropic average σ_{iso}^{NMR} and the anisotropy Δ^{NMR} .

- The HB depletion of the electron density around the proton affects σ_{iso}^{NMR}, whereas the acceptor oxygen electrons induced magnetic field perturbs the anisotropy.

Water

- *The shielding anisotropy has been measured in ice; in the liquid, $\hat{\sigma}^{NMR}$ is averaged by fast molecular tumbling and only its isotropic part can be determined. Being the isotropic shielding reference value, $\sigma_{iso}^{NMR,ref}$ available in an absolute scale the shielding isotropic part σ_{iso}^{NMR} can be directly obtained (Eq.2).*
- *Well different may be the situation in the deep supercooled regime and for amorphous water (LDA and HDA) where the effects of the growing HB network are detected.*
- *In the liquid water stable phase the HB life-time is of the order of some picoseconds, but on going toward the amorphous phase, by supercooling it increases of many orders of magnitude with an additional increase in the HB network stability and also in its size. Hence the HB network influences NMR tensors (δ and σ) and is detectable.*
- *Liquid water has the polymorphism observed in its glass phase: there are two water forms one is that of the HB network characterized by a low density, the LDL, and a remaining disordered , HDL, with an higher density. The LDL increases in size and stability on decreasing T and is at the basis of the water anomalies.*
- *These structural effects can be directly determined in the deep supercooled water by means of the asymmetries in the NMR line-shapes rather than from its second-order contribution to the 1H spin relaxation rate.*

The measured NMR water chemical shift

NMR

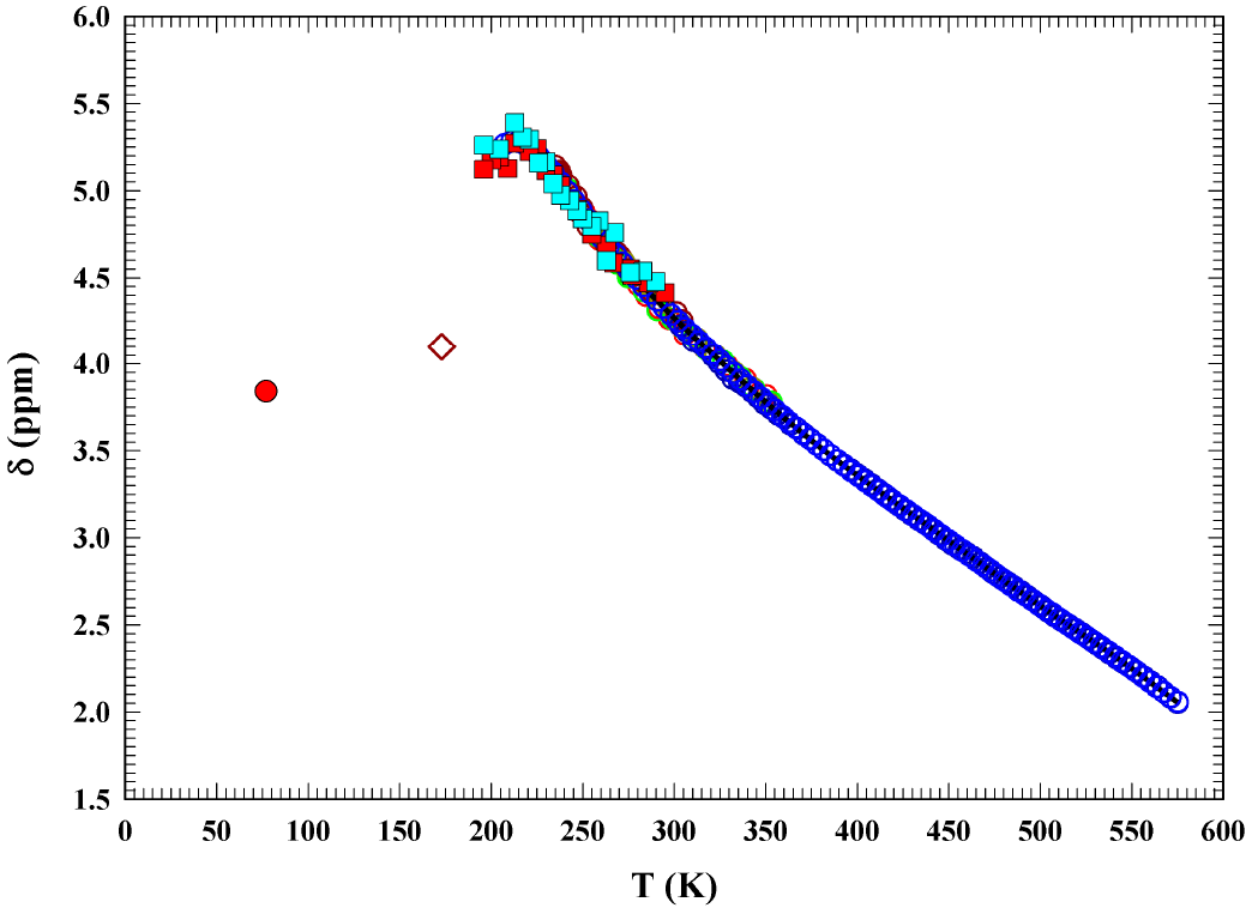

The water chemical shift (δ) in a T interval ranging from the critical region to the deep supercooled regime. The data of bulk water and inside large capillary and emulsions, are reported as blue symbols; whereas data of nanotubes confided water, ice and poly-ice are reported in different colors.

Nuclear Compton Scattering (NCS)

Deep inelastic Neutron scattering (DINS) is a spectroscopic technique based on neutron energy and momentum transfers large enough to satisfy the Impulse Approximation (IA).

Spectra collected in Time-of-Flight (ToF) mode and for the forward scattering angle (q) show different peaks due to the mass-selection capability of DINS measurement.

The broadening of each peak is related to the mean kinetic energy $\langle E_K \rangle$ of each atom in the system and the peak itself named neutron Compton profile (NCP) represents the nuclear momentum distribution (NMD).

In the water case, two main peaks are observed and from each *j-th* detector and a NCP for the hydrogen nuclei is obtained as $F_J(y, q)$, where y is a scaling variable.

The position of the experimental peaks follows the atoms recoil lines and it varies for each scattering angle and detector.

NCS

The NCS theory is well established.

Within the IA, the double-differential scattering cross section and the dynamic structure factor ($S(q;\ \omega)$) can be factorized to a function $C(E_1;E_2;\phi)$, depending on the experimental setup (scattering angle ϕ, incident and scattered energies E_1 and E_2) and the Compton profile function $J(y,\hat{q})$ as:

$$S(q,\omega)\frac{\hbar q}{M} = J(y,\hat{q}) = \int n(p)\delta(y - p\cdot\hat{q})dp,$$

$$\frac{\partial^2\sigma_M}{\partial\Omega\partial E_2} = C(E_1;E_2;\phi)J(y,\hat{q}) = b^2\frac{M}{\hbar q}\left(\frac{E_2}{E_1}\right)^{\frac{1}{2}}J_{1A}(y,\hat{q}),$$

$$y = (M/q)\left[\Delta E - (q^2/2M)\right]$$

y is the West scaling variable representing the projection of the particle momentum distribution n(p) along the $\hat{q}$ direction; and M the mass, b the scattering length of the nucleus, $\hat{q}$ the scattering transfer momentum and $\hbar$ the Planck constant. This relations also reflect the conservation laws of the momentum and energy.

Due to the finite q values in the scattering process, the instrumental resolutions $R_l(y;q)$ and the signal broadening for each *l-th* detector (final state effects $\Delta J_l(y;q)$), the measured NCP functions are:

$$F_l(y;q) = [J(q) + \Delta J_l(y;q)]\otimes R_l(y;q).$$

To derive $n(p)$, the $F(y,q)$'s can be respectively expressed in terms of Gauss-Hermite (GH), $n_{GH}(p)$, or of a Multivariate Gaussian momentum distribution, $n_{MG}(p)$.

The obtained line-shapes ($J_{GH}(y)$ and $J_{MG}(y)$) are a combination of the anisotropy parameters $\sigma_{NCP,i}$ (the deviation of the p distribution along the space directions $i = x; y; z$) yielding: $\sigma^2_{NCP} = (\sigma^2_{NCP,x} + \sigma^2_{NCP,y} + \sigma^2_{NCP,z})/3$.

Any local order variation corresponds to changes in these NCP line-shape.
As a consequence there will be a difference $\Delta_{NCP} = \sigma_{NCP,2} - \sigma_{NCP,1}$ between the σ_{NCP} final (2) and initial (1) values.

σ_{NCP} mirrors the anisotropy in the momentum distribution.

σ_{NCP} can be also intended as the system global variable, centered along the H recoil line and represents the H momentum along the direction of the transferred neutron momentum.

In the y space, all hydrogen NCP are centered at the same $y = 0$ value with the same width σ_{NCP}, and $\langle E_K \rangle = 3\hbar^2\sigma^2_{NCP}/2M$.

With these parameters n(p) can be projected onto the three molecular axes yielding the directional values of σ_{NCP} and mean kinetic energy ($\langle E_K \rangle_i, i = x; y; z$).

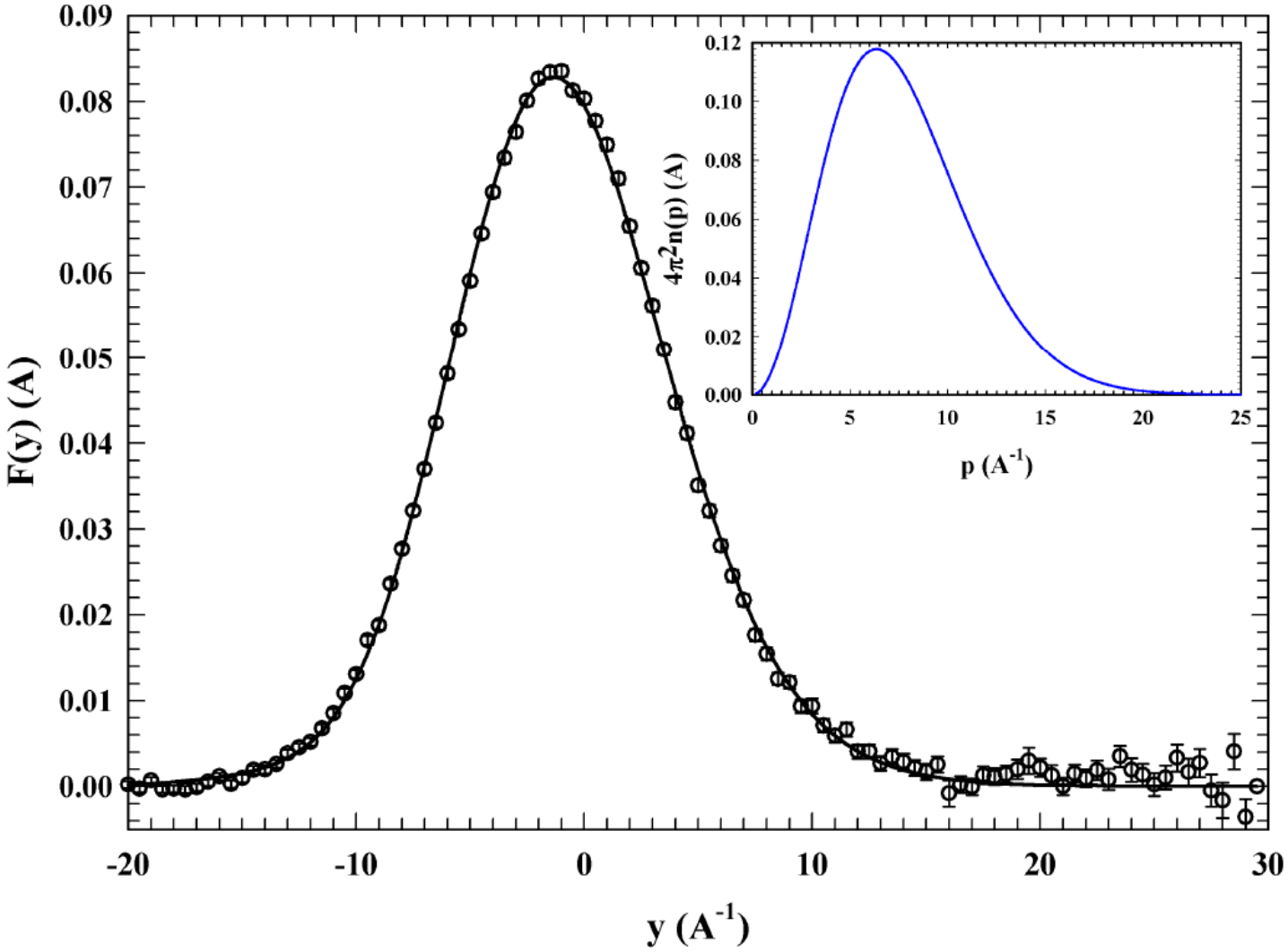

The angular average NCP for water, $F(y)$, for T = 300 K. The resulting best fit, obtained according to the described procedure, is illustrated as a continuous line.

In the inset the calculated momentum distribution ($4\pi^2 n(p)$) versus the momentum p.

At this stage it becomes important to stress that both the DINS and the NMR deal with the system nuclear distribution; so that the local order experienced with the two techniques, under the same thermodynamical conditions, is the same.

Therefore although the interaction radiation matter has different potential, the response in terms of the scattering matrix is the same.

Hence both the shielding tensor (NMR) and the momentum distribution (NCP) give the same response to the respective induced perturbation on the system: both provide the same measure of the system asymmetries.

Configurational data obtained by using one of the two techniques can be used to describe the findings of the other one, or to confirm the completeness of the results.

Rather than to a direct measure of the HB length and angle (and their correlations), both σ_{NCP} and σ_{iso}^{NMR} represent the water anisotropy although probe the system nuclei by means of different radiation matter coupling, but at different wave-vectors.

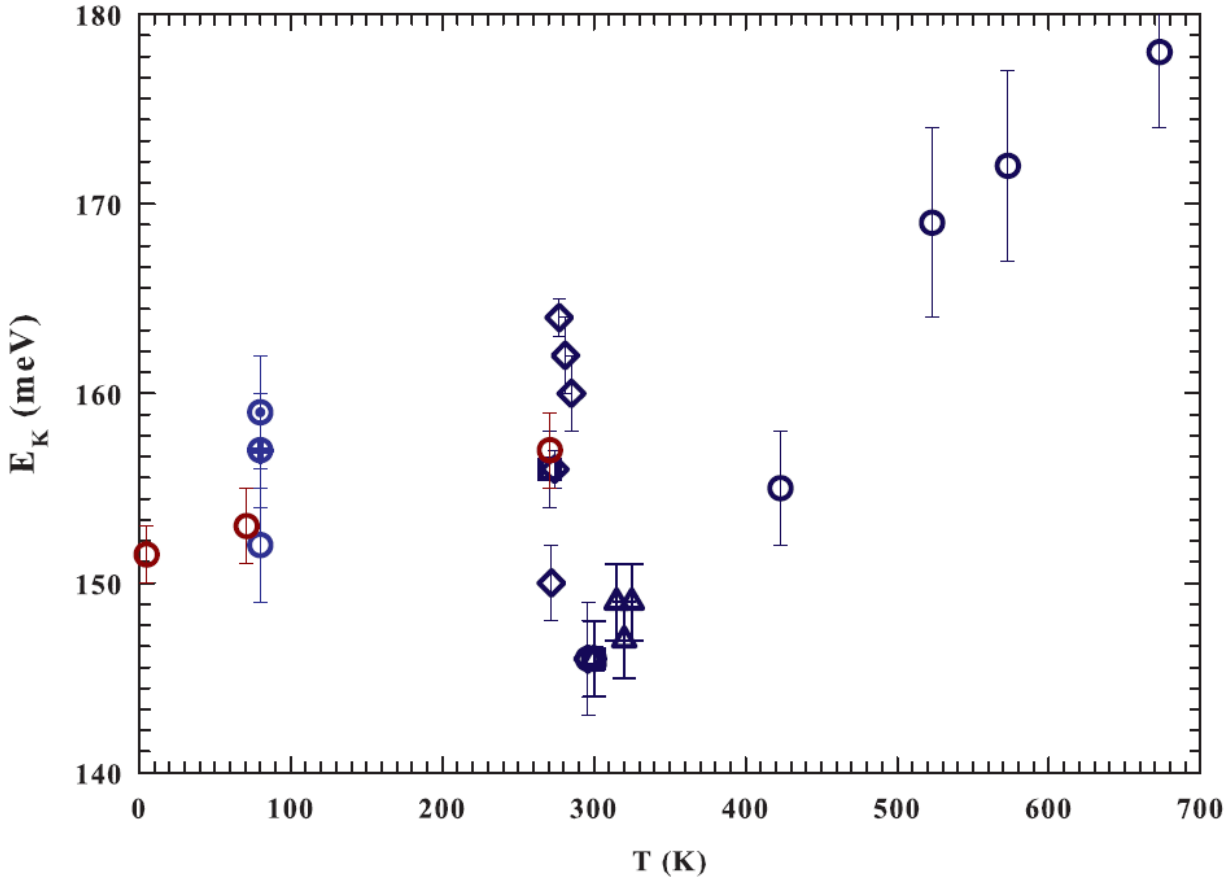

The $\langle E_K \rangle$ obtained from the corresponding $F(y;q)$ in the liquid and supercritical phases together with several types of ices.

From the super-critical region, a T decrease behaves a continuous decrease in $\langle E_K \rangle$ up to about 310 K, below which a marked increase on approaching the supercooled liquid phase is shown. From the supercooled liquid temperature to those of the amorphous ices, $\langle E_K \rangle$ decreases slowly and evolves to the lowest temperatures on approaching values (within the experimental error) of the order of 155 meV.

Such a situation can be due to the onset for T □ 310 K of a change in the molecular local order connected with the onset of a dynamics involving some water molecules: i.e. the water tetrahedral network.

Independently, by the coupling potential with the nuclei, the essential difference between the NMR, NCS (and XCS) is in the used wave-vector (and thus the wave-length).

More precisely, whereas in the NMR case is q ≡ 0, in the neutron scattering case q ≠ 0.

Hence, the NMR averages the local order and anisotropy on a more large length scale (mesoscopic) than the NCS, this latter instead looks at short to moderate lengths of the microscopic molecular order.

Such a situation is clarified in the next Figure where both σ_{NCP} and σ_{iso}^{NMR} are illustrated as a function of the temperature. Essentially, these anisotropy functions differ in value only for a multiplicative factor.

However, the T evolution of these two quantities is, within the experimental error, the same in the range 320 < T < 600 K; σ_{NCP} and σ_{iso}^{NMR} decrease practically with the same rate as T decreases.

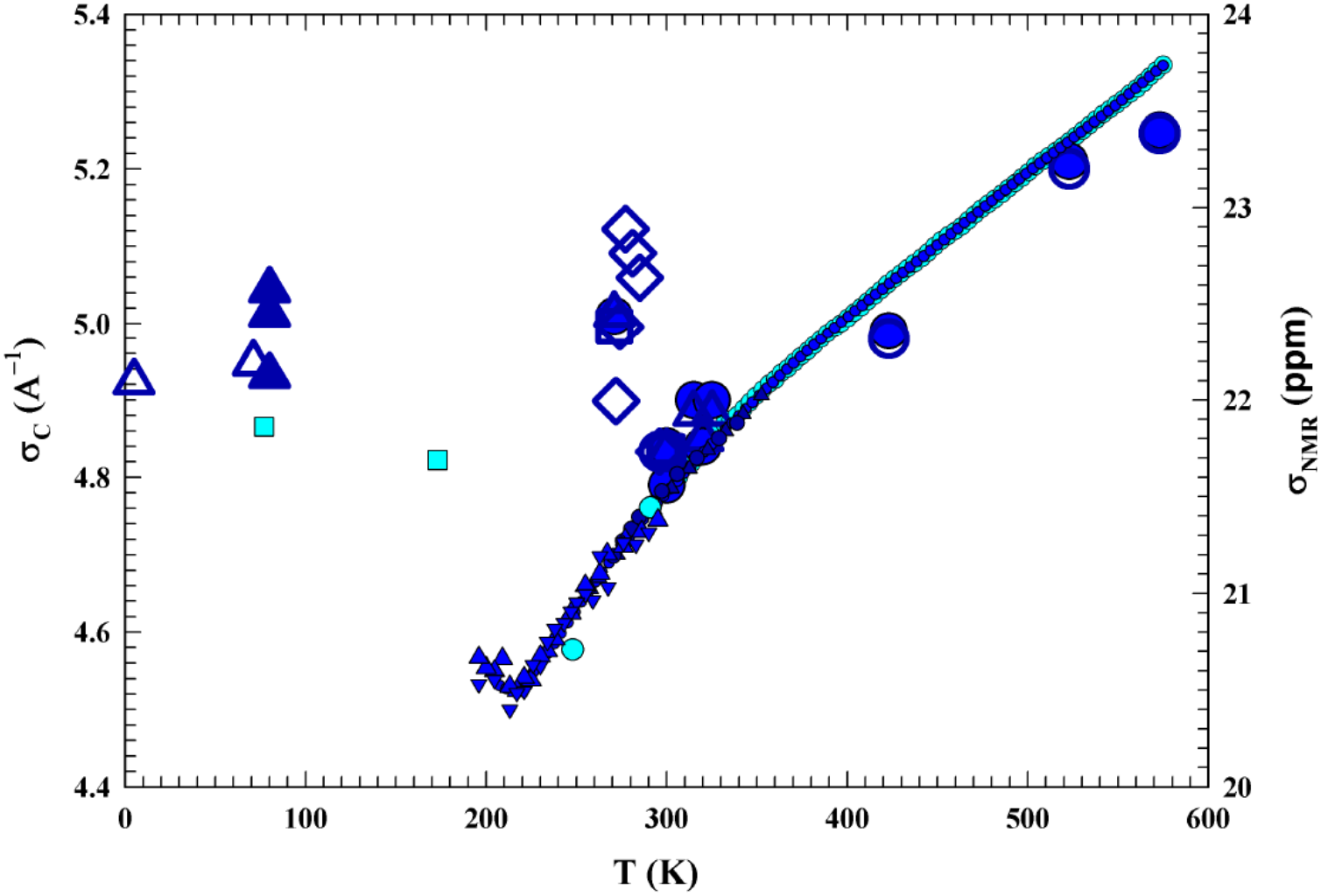

The temperature behavior of $\sigma_{NCP}(T)$ (left scale) and $\sigma_{iso}^{NMR}(T)$ (right scale). σ_{iso}^{NMR} is obtained from the chemical shift data (smaller symbols) whereas the NCP data (bigger symbols) are obtained from the mean kinetic energy $\langle E_K \rangle$.

FINDINGS a

A marked difference is observed in the low T regime: σ_{iso}^{NMR} decreases with continuity well inside the very supercooled regime showing a minimum for T ~220 K, after that it seems to evolve toward the ice.

Instead, σ_{NCP} behaves as the $\langle E_K \rangle$: a marked increase at about 310 K, and after a moderate decrease on going toward the lowest temperatures. Practically, in the deep supercooled phase both the anisotropy functions evolve on decreasing T to the values of the corresponding ice forms.

The differences in the σ_{NCP} and σ_{iso}^{NMR} by decreasing temperature, are accounted for their different working wave-vectors.

It is of special interest that in the Compton case the singularity in σ_{NCP} is observed around 310K. In the NCS it is q ≠ 0 (27 < q < 230 $^{\circ}$Å^{-1}) a condition where DINS experiments explore microscopic length.

Hence if the system changes its properties (dynamics or structure) inside this length scale, the response function ($S(q,\omega)$ or $J(y)$) must change correspondingly by reflecting such a situation.

FINDINGS b

At the σ_{NCP} singularity, lies the temperature T* of special interest for water and related with the onset of the water LDL phase, where HDL molecules dominate the system thermodynamics.

Instead, the NMR probe (q ≡ 0), working on macroscopic lengths, will be insensitive to the onset of this HB structure.

Hoewver, when the LDL water network dominates the HDL phase and its characteristic size evolves toward the mesoscopic size, the technique will becomes sensitive to it and presents the observed minimum.

In the past this was explained under the assumption that the NMR chemical shift probes the local order so that according to the entropy definition, the configurational specific heat can be calculated from δ(T).

Such a quantity has a maximum at ~225 K i.e., where the HB network is fully realized, with the LDL phase dominating the HDL one, and the water thermodynamics is characterized by maxima in the response functions fluctuations (Widom line).

Conclusion

The local order of liquid water, from the supercooled to the superheated regime, and in different ices and glasses has been evaluated through the nuclear momentum distribution, σ_{NCP} of the Hydrogen NCP lineshapes.

At the same time, the isotropic part of the shielding tensor σ_{iso}^{NMR} was separately obtained by means of a NMR experiment.

Our data support the idea that the shielding tensor (NMR) and the momentum distribution (NCP) provide the same response to the induced system perturbation by providing the same measure of the asymmetries.

The basic difference is however in the ”resolution properties” of the two techniques. Whereas NCS working with a finite wave-vector will be sensitive to the microscopic scale, the NMR working at q= 0 can detail the system properties only in the mesocopic sizes.

Thus the σ_{iso}^{NMR} gives evidence in the very deep temperature regime of the onset of the Widom line.

Finally, the NCP spectra confirm the singular temperature, T*, as the locus of the onset of the tetrahedral structure (LDL phase).

A lot of Thanks

The thermal evolution of the NMR magnetization M(T,ν) spectra in a thermal cycle.

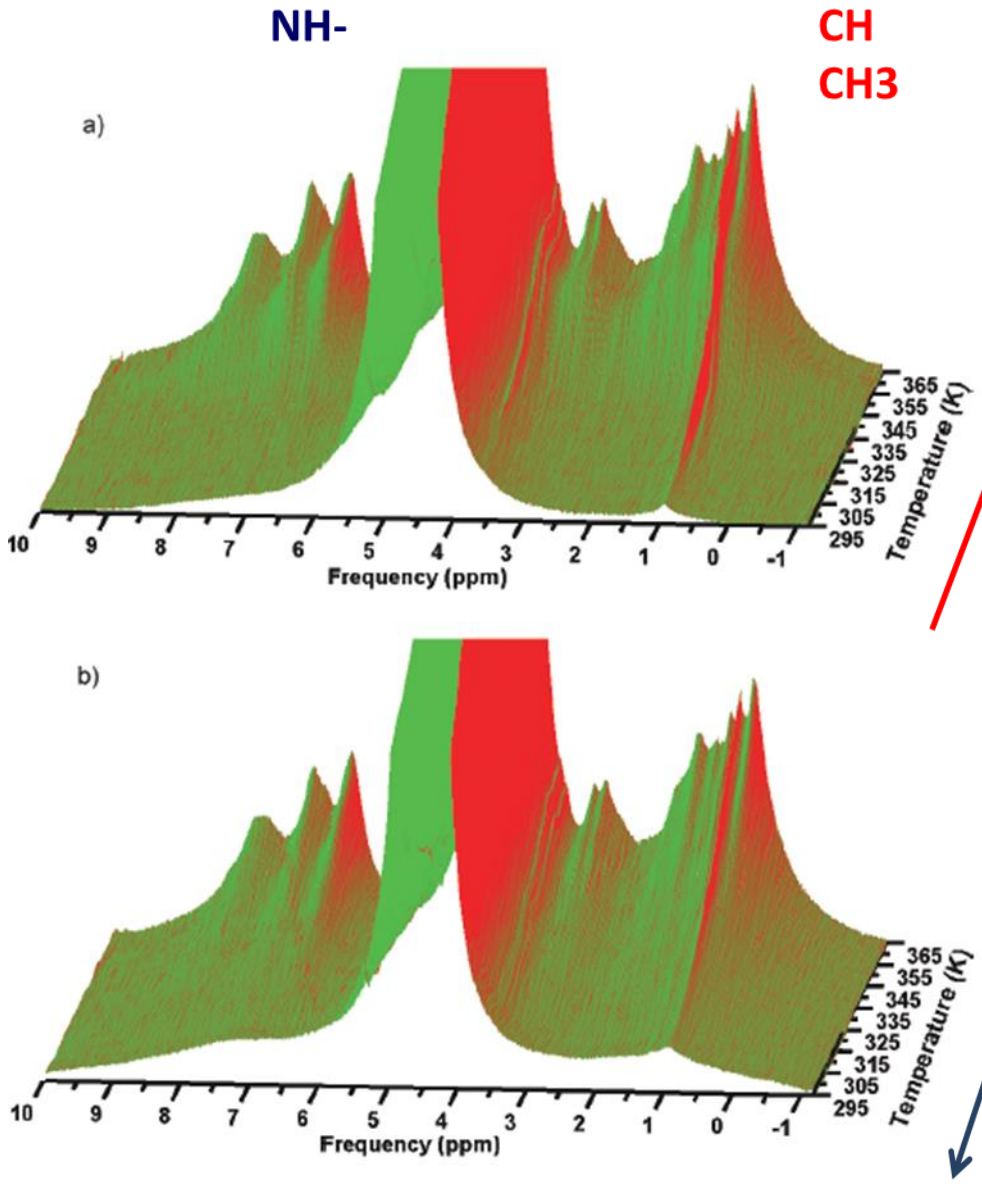

The hydrated lysozyme unfolding reversible/irreversible detected by the NMR technique.

The study of the protein (hydrophobic and hydrophilic) metabolites in a thermal cycle.

The study was an experimental proof of the protein funnel (energy landscape).

F. Mallamace et al PNAS, 2016, 105 536

Hydrophilic Groups (NH)

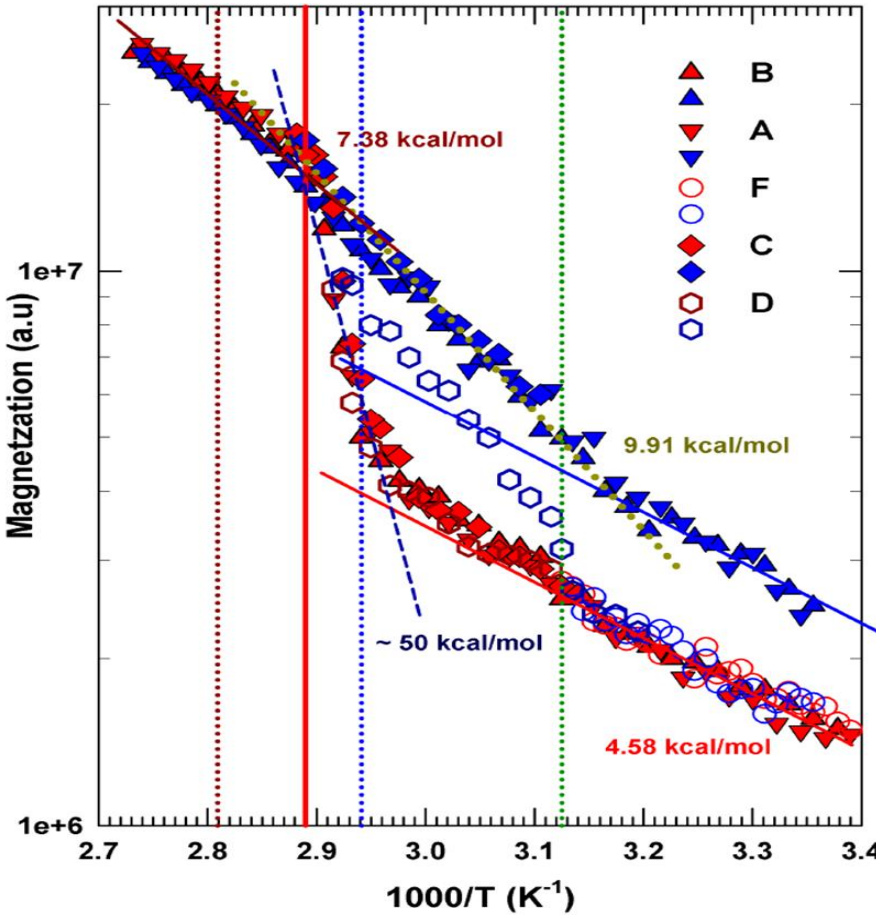

Hydrophobic Groups (CH)

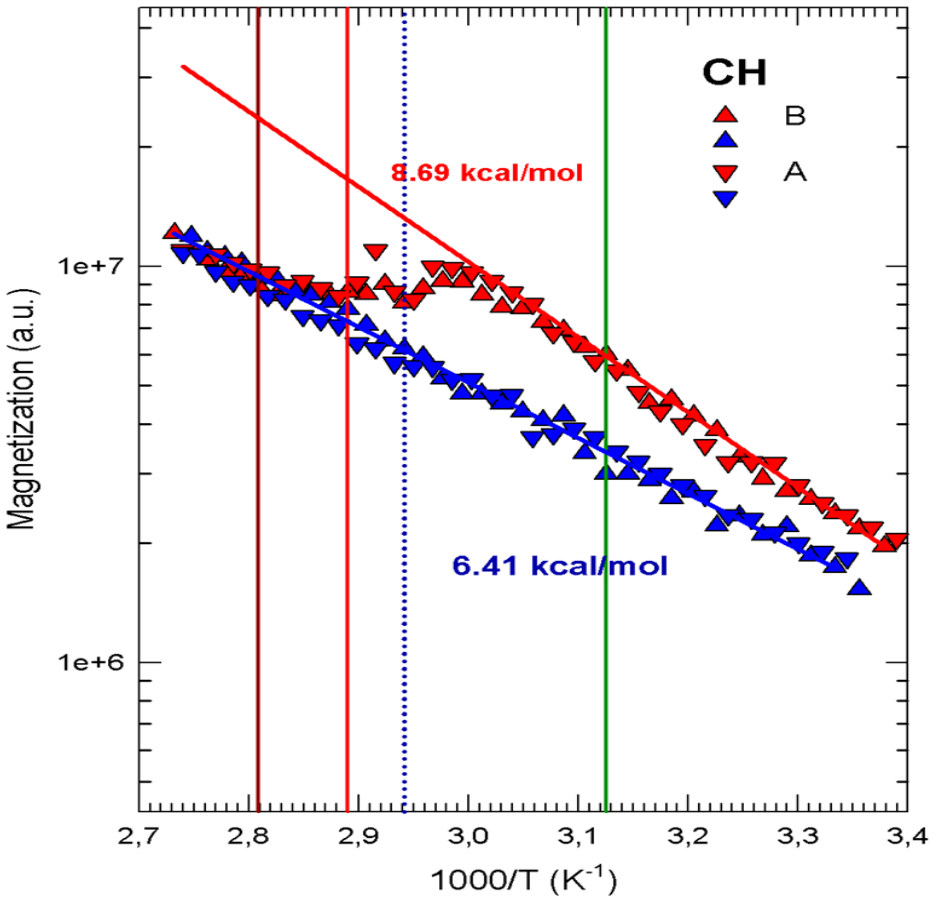

Although the hydrophobic effect has the same importance of the hydrophilic one, a reasonable understanding of its properties is far to be achieved!

***Hydrophobic moieties are amphiphilic, polymer, colloid, polyelectrolyte, biological molecules, etc.; of large importance in many fields of science and technology.**

****Hydrophilicity is fully described by means of the HB interaction, but on despite of the many attempts, we do not have analytical forms to treat quantitatively hydrophobicity.***

E.g. a complete experimental measurement of the pair distribution function $g_{AA}(r)$ between hydrophobic molecules (A), and therefore the corresponding potential of mean force $W(r)=-k_BTln\ g_{AA}(r)$ between the two hydrophobic molecules was never obtained.

***From one side is of great interest to understand the forces underlying hydrophobic interactions, but at the same time to evaluate all the interesting implications such forces have.**

***An important issue is that the hydration shells near a hydrophobic solute can also affects (due to the hydration forces) the structure of the solute itself.**

This latter process certainly can have a great scientific relevance because solute molecules can assume dipole moments, with significant changes on the solution by changing the thermodynamic variables.

ACTUAL INFORMATION:

a) NMR experiments for water in hydrophobic nanotubes suggest a hydrophobic-hydrophilic transition upon cooling from 22°C to 8°C. The structure of interfacial water on hydrophobic surfaces could be T dependent.

HJ. Wang, X.K.i Xi, A. Kleinhammes, Y. Wu", Science 2008, 322 80-83.

b) On the purely theoretical side, not trivial solute-solvent effects (and viceversa) on their structure and energetic of the solvent are schematically predicted.

D. Ben-Amotz , B. Widom PNAS 2006, 50 18887, J. Phys. Chem B 2006, 110 19839. B. Widom, P. De Gregorio J. Phys. Chem, C 2007 111, 16060.

The NMR of: a) Water and b) Water-Methanol relaxation times

T_1 spin-lattice (longitudinal)

T_2 spin-spin (rotational)

These times can be explained at nuclear level by two approaches developed by Bluembergen, Purcell, Pound (BPP) and Kubo, Tomita, Hubbard (KTH) that allows the correlation times calculation, coming from the effects of the thermal motion of the magnetic nuclei upon the spin-spin interaction.

N. Bluembergen, E.M. Purcell and R.V. Pound, Phys. Rev., 73, 679 (1948). R. Kubo and K. Tomita, J. of the Physical Soc. of Japan, 9, 888 (1954). P.S. Hubbard, Phys. Rev. 131, 275 (1963).

The bulk water NMR spin-lattice (T_1) and spin-spin relaxation times (T_2).

Actual and literature data.

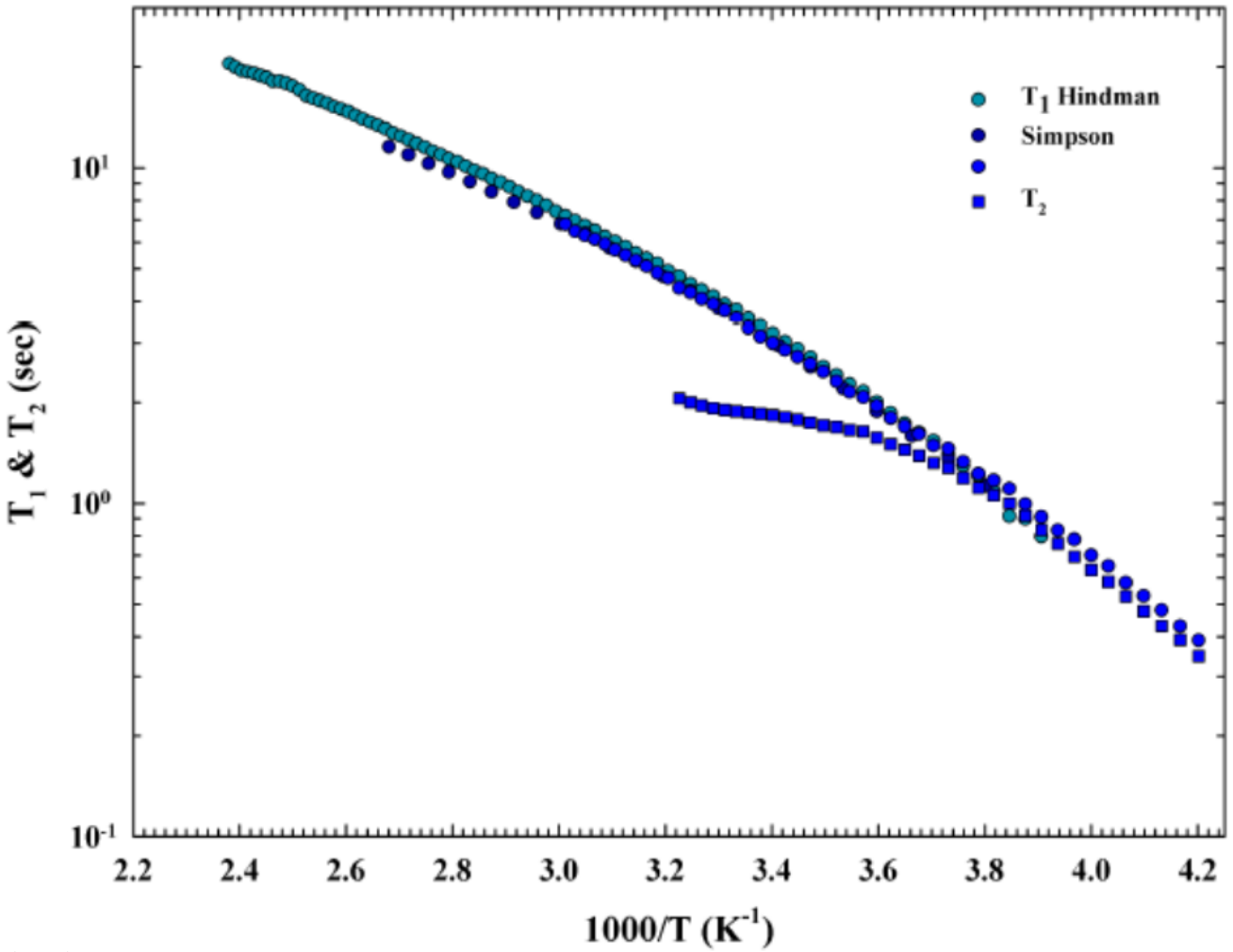

J.C. Hindman, J. Chem. Phys . 60, 4488 (1974);
J.H. Simpson and H.Y. Carr, Phys. Rev. 111, 1201 (1958);

In the BPP approach to NMR spectroscopy, after the exposure to the perturbing radiation, the system tends to upset the original equilibrium state, by equalizing the population of the various quantum levels.

The effect of the nuclear motion on the dipolar broadening, can be treated as a sort of random modulation of dipolar field owing to the Brownian motion of the atomic nuclei.

The spin-lattice time, T_1, represents essentially how long one must wait, after the application of the constant field H_0, for the establishment of thermal equilibrium. It is :

$$(1/(T_1))=(3/2)\gamma^4\hbar^2 I(I+1)\sum_i J_i(i\nu_0)$$

where γ is the gyromagnetic ratio of proton, $2\pi\hbar$ is the Planck constant, I the spins energetic levels, $\omega_0/2v=v_0$ is the Larmor frequency, and J_i the spectral components.

If the intermolecular effects are negligible and the system is dominated only by the dipole-dipole interaction, T_1 will be:

$$(1/(T_1))=(3/2)\ \gamma^4\hbar^2 I(I+1)[J_1(v_0)+(1/2)J_2(2v_0)] \qquad (1)$$

so that $1/T_1$ can be divided into two parts $(1/T_1=(1/T_1)_{v_0}+(1/T_1)_{2v_0})$ corresponding to the single spin- and double spin-inversion processes, each part is expressed by the corresponding J_N.

For water by considering only the effect on a given proton of its nearest neighbor (the other one in the H_20 molecule) and by assuming that:

i) the molecule as rigid

ii) the orientation of the vector connecting the two protons varies randomly, without preferred directions,

the BBP model proposes that the measured ^1H T_1 is determined by interaction fluctuations, induced by molecular motions, characterized by only a correlation time τ_c. "These fluctuations are the effects of the thermal motion of the magnetic nuclei upon the spin-spin interaction (the local Brownian motion closely related to the characteristic time of the Debye's theory of polar liquids)." Hence:

$$1/T_1 = (3\gamma^4 \hbar^2/10r^6)(J_1 + J_2) \qquad (2a)$$

with

$$J_1 = (\tau_c/(1 + (\omega_0 \tau_c)^2)) \quad \text{and} \quad J_2 = (4\tau_c/(1 + 4(\omega_0 \tau_c)^2)) \qquad (2b)$$

***r* represents is the inter-proton distance.**

****There is also a relation between τ_c and the nuclear Larmor frequency if this latter quantity is much less than $1/T_1$ the perturbations caused by the local field nearly average out, and the width of the resonance line, in frequency will be ~ τ_c.**

Lately, the NMR absorption has been reconsidered by Kubo&Tomita for a general expression for the frequency-dependent susceptibility $\chi_H(\omega)$, in terms of a quantum-statistical method.

Such a method is based on the theory of irreversible process by considering the system Hamiltonian as the sum of a "secular" terms that commutes with the unperturbed terms plus a "non-secular" part of the perturbation.

Secular and non-secular contributions lead to different spectral functions J_i with different relaxation times τ_i . Only in the case of a system relaxing between two energetic levels there is a single relaxation time τ_c.

In the ideal case of isotropic nuclear arrangements, the two kinds of spin inversion processes have different weights for the spin-lattice relaxation: the secular one is represented by the BBP Eq. 1, whereas the non-secular broadening effect is

$$1/T'_1 = \gamma^4 \hbar^2 I(I+1)[15/4 J_1(\nu_0) + 3/8 J_2(2\nu_0)] \quad (3)$$

Generally, $T_1 \neq T'_1$.

The model give also a proper evaluation for the spin-spin relaxation time

$$T_2 \; (1/T_2 = \gamma^4 \hbar^2 I(I+1)\tau_0 + 1/T'_1)$$

that in the ideal case in which all the relaxation times corresponding to the different spectral functions are identical to τ_c, is:

$$1/T_2 = (3\gamma^4 \hbar^2/20r^6)(3\,\tau_c + 5J_1 + J_2/2) \quad (4)$$

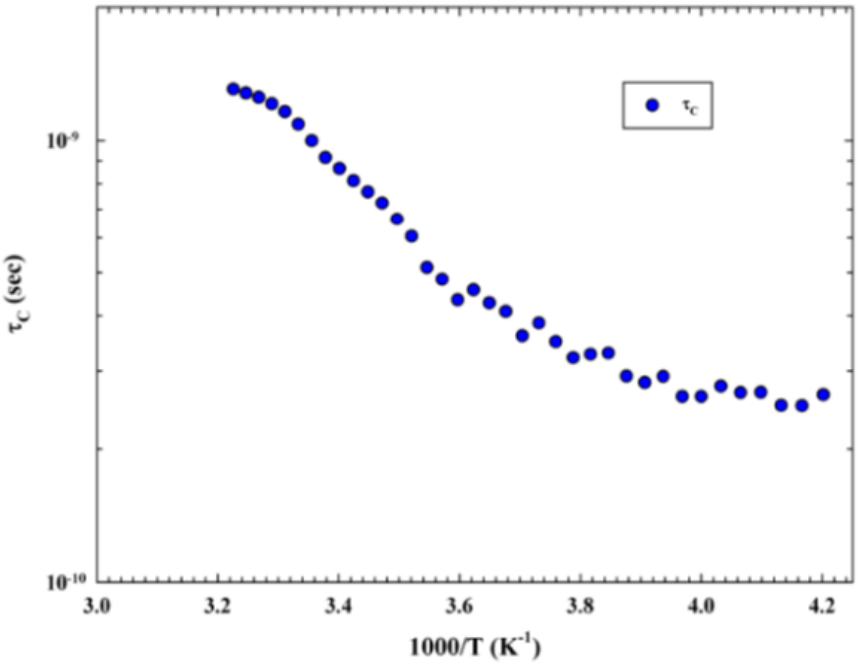

The Arrhenius plot of τ_c evaluated by means of the Eq. 2 and 4

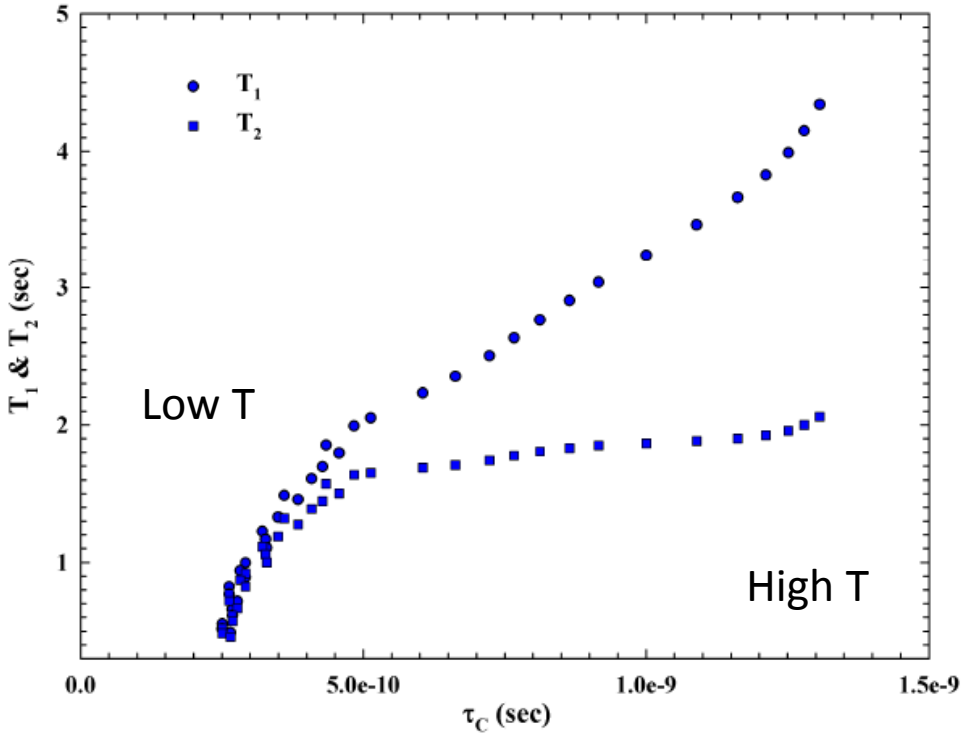

The Bluembergen, Purcell and Pound analisys of T1 and T2 vs τ_c

The KT approach have suggested a new way to treat the T_1 data* by assuming that to the observed protons relaxation contribute three terms: two dipolar (intermolecular (D-inter), and intramolecular (D-Intra)) and the nuclear spin-rotation interactions (SR):

$$1/T_1 = 1/T_1^{D\text{-}inter} + 1/T_1^{D\text{-}intra} + 1/T_1^{SR}$$

The rotational nuclear if compared with the dipolar one is smaller; for water case may be evaluated only for $T \geq 350$ K (strongly contributes to the system dynamics in the region of the critical point) **. Therefore:

$$1/T_1^{D} = 1/T_1^{inter} + 1/T_1^{intra}$$

On these bases Hubbard proposed that the intermolecular dipolar contribution is strongly related with the molecular self diffusion coefficient D_S :

$$1/T_1^{inter} = N\pi\gamma^4\hbar^2/(5aD_S))[[1+0.233((b/a))^2+0.15((b/a))^4+ \ldots]$$

Thus having D_S such a contribution can be evaluated and from the measured T_1 we can have $T_1^{D\text{-}intra}$, that under the condition $1/\omega_0 \gg \tau_i$, can be written *** in terms of the system viscosity , or as a molecular rotational time τ_θ :

$$1/T_1^{D\text{-}intra} = (3\gamma^4\hbar^2/r^6)\,\tau_\theta$$

*D.W.G. Smith and J.G. Powles, J. Mol. Phys. 10, 451 (1966); P.S. Hubbard, Phys. Rev. 131, 275 (1963); **T. DeFries and J. Jonas, J. Chem. Phys. 66, 896 (1977); *** E. Lang and H.D. Ludemann, J. Chem. Phys, 67, 718 (1977).

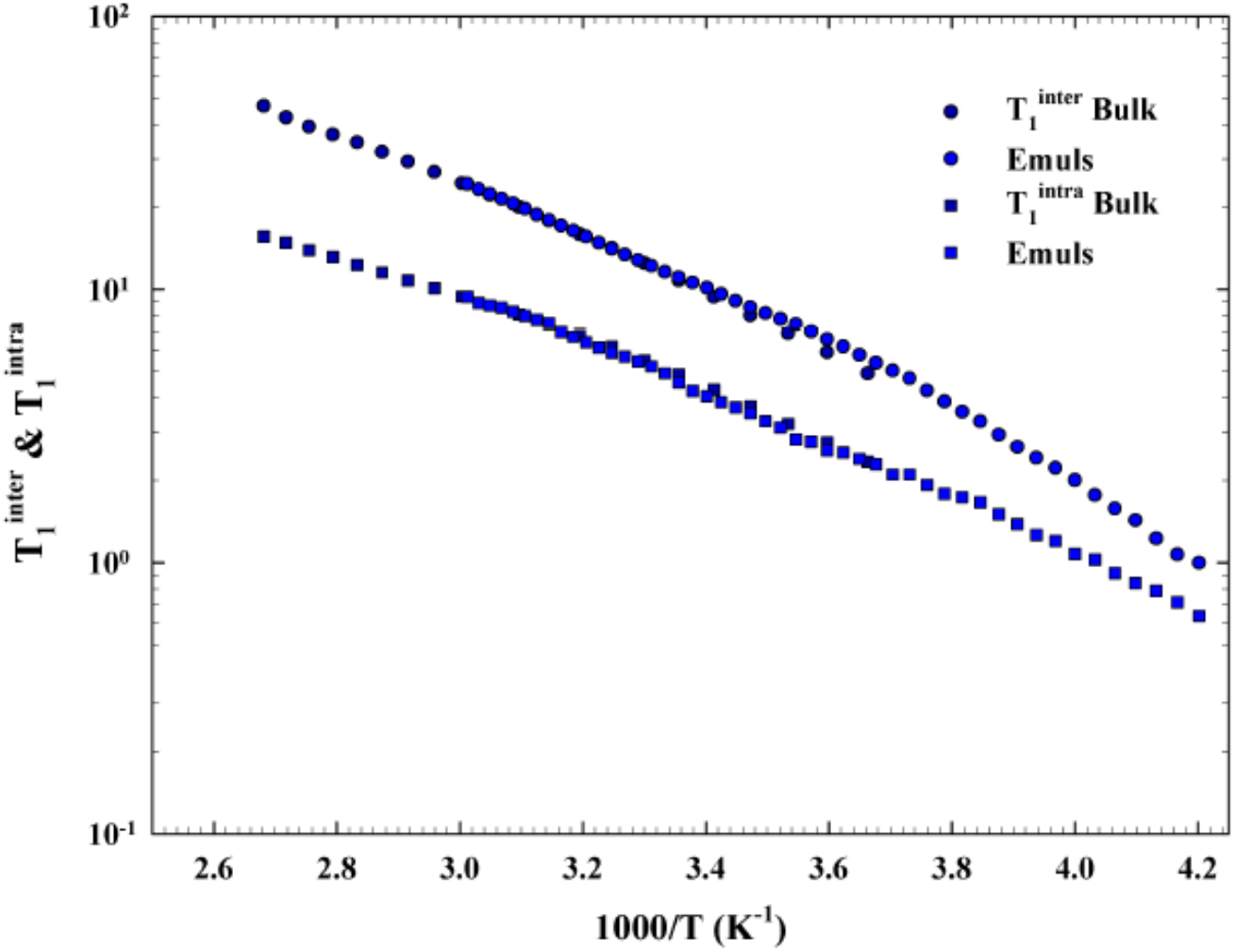

The T_1^{inter} and T_1^{intra} of bulk and emulsioned water.

ESI-2016

The bulk and emulsioned water τ_θ coming from the present experiment and literature data in an Arrhenius plot; are also reported (properly scaled) the viscosity and the relaxation times coming from depolarized Rayleigh Scattering experiments.

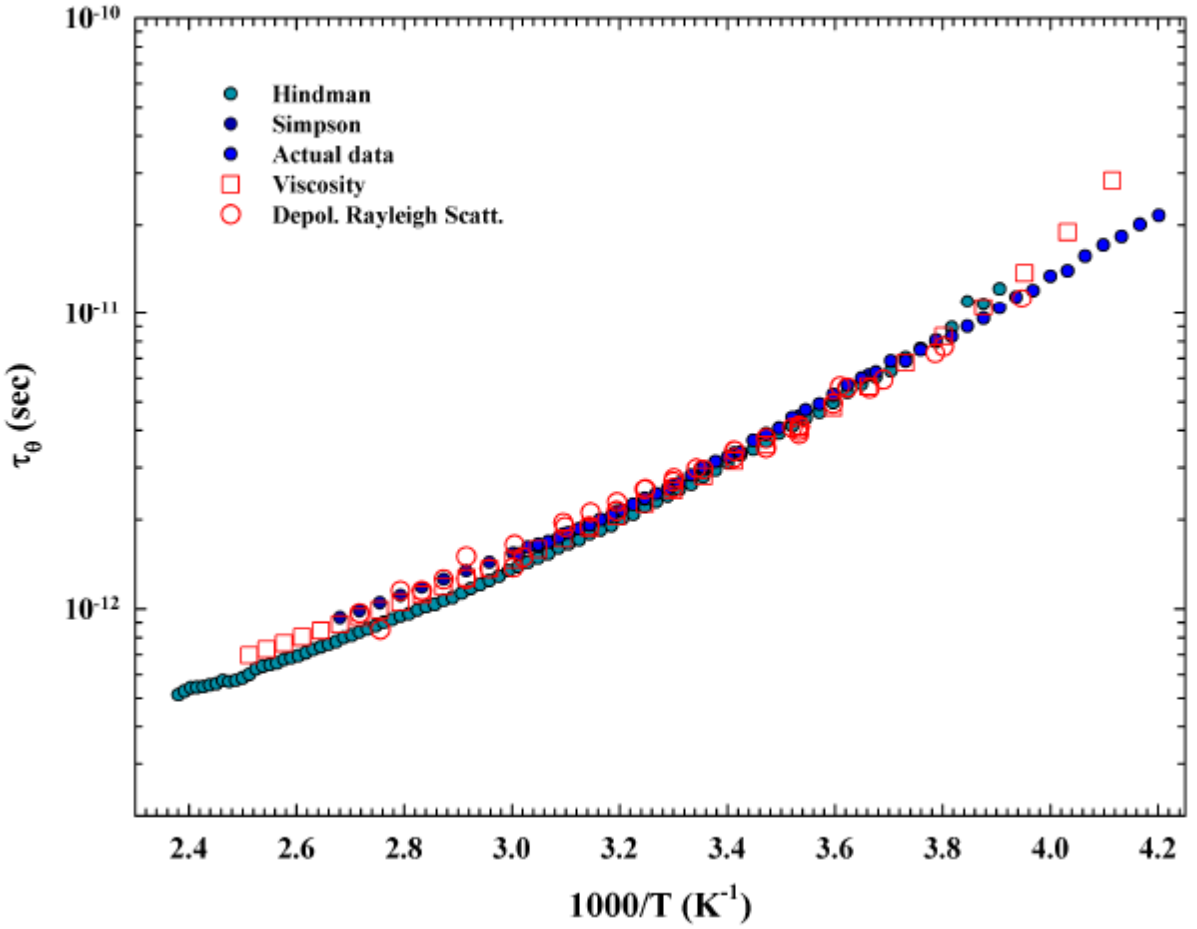

J.C. Hindman, J. Chem. Phys . 60, 4488 (1974); J.H. Simpson and H.Y. Carr, Phys. Rev. 111, 1201 (1958); C. H: Cho et al, J.Phys. Chem. B 103, 1991 (1999; V. Mazzacurati et al. J. Chem. Phys. 93, 7767 (1990); M. Paolantoni et al. J. Chem. Phys. 127, 024504 (2007).

ESI-2016

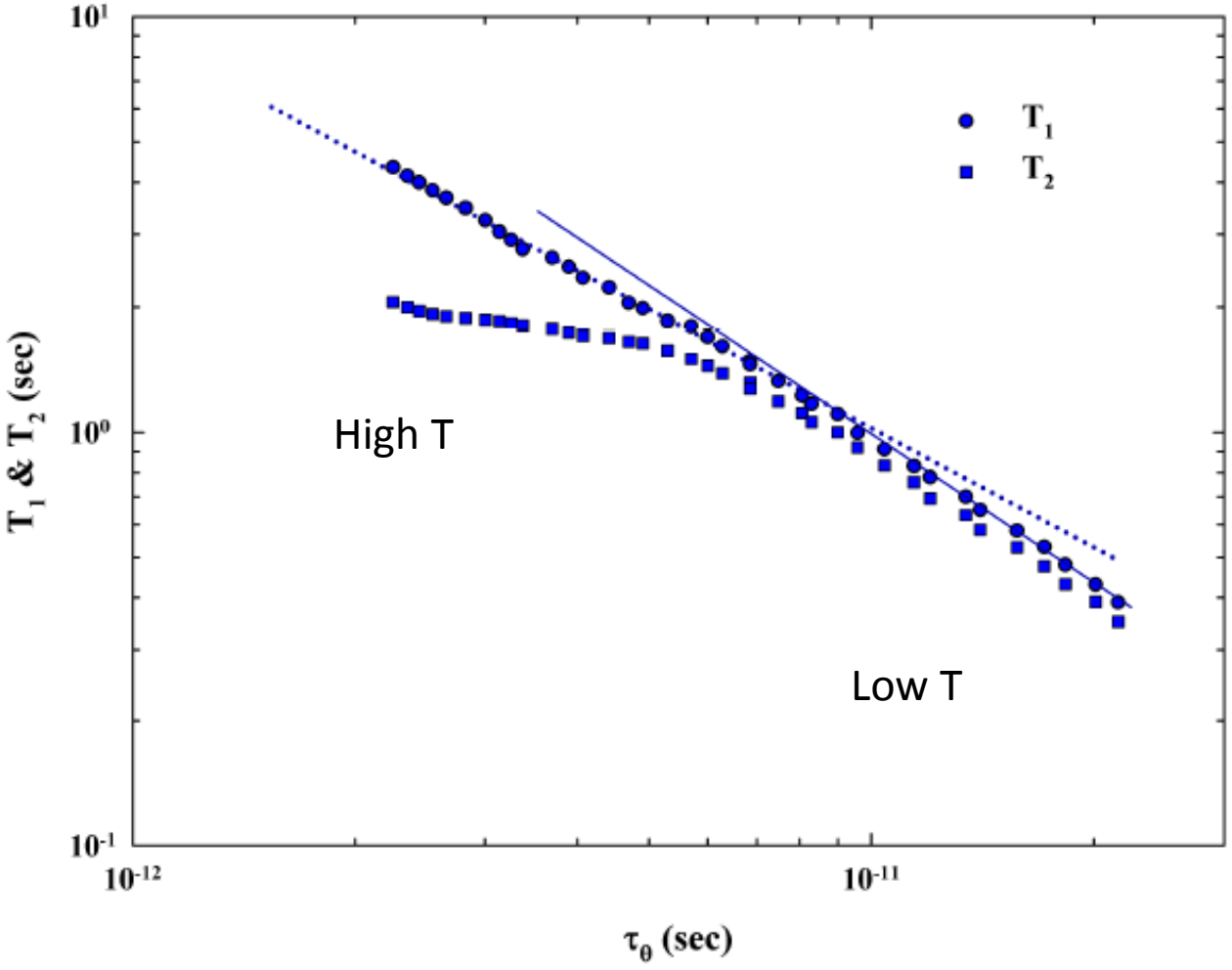

Full correlation in the low temperature regime dominate by the OH network, a well different behavior for T ≈ 270 where the HB life-time is of the order of picoseconds.

Water and Methanol

NMR allow to study separately the behaviors of the hydrophilic (hydroxyl) and hydrophobic parts of the same molecule (methyl):

OH water
OH methanol
CH3 methanol.

Here we report their evolutions in water-methanol mixtures as a function of the concentrations (methanol molar fraction X_M) and temperature.

An Arrhenius plot of the spin-lattice (T_1) and spin-spin relaxation times (T_2) for water, methanol and their solutions at the different concentrations (methanol molar fracion). In the top and in middle panels the water (OH_W) and methanol (OH_M) hydroxyls, respectively . The bottom panel report data of the methanol methyl group (CH_3).

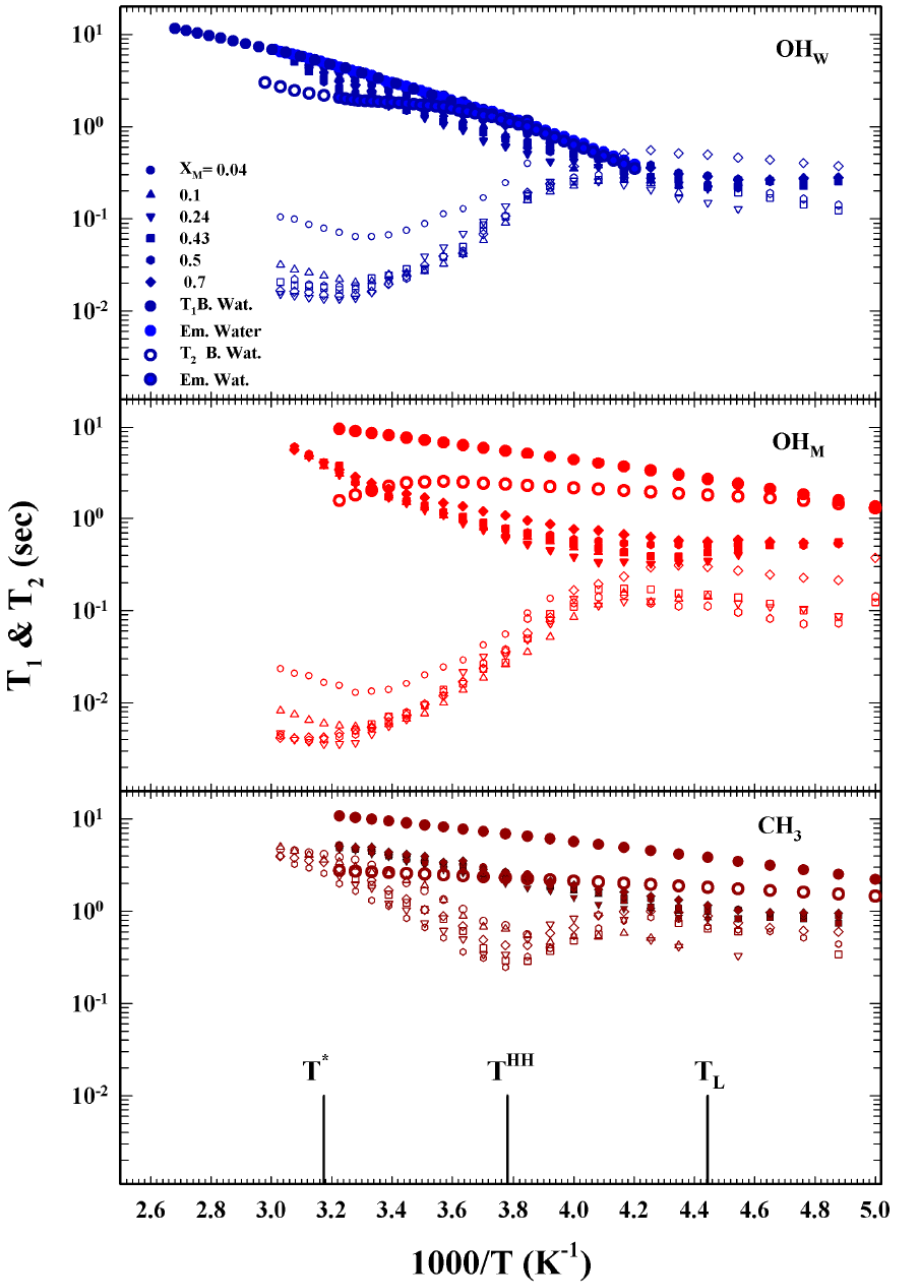

ESI-2016

An Arrhenius plot of all the measured spin-spin relaxation times (T_2)

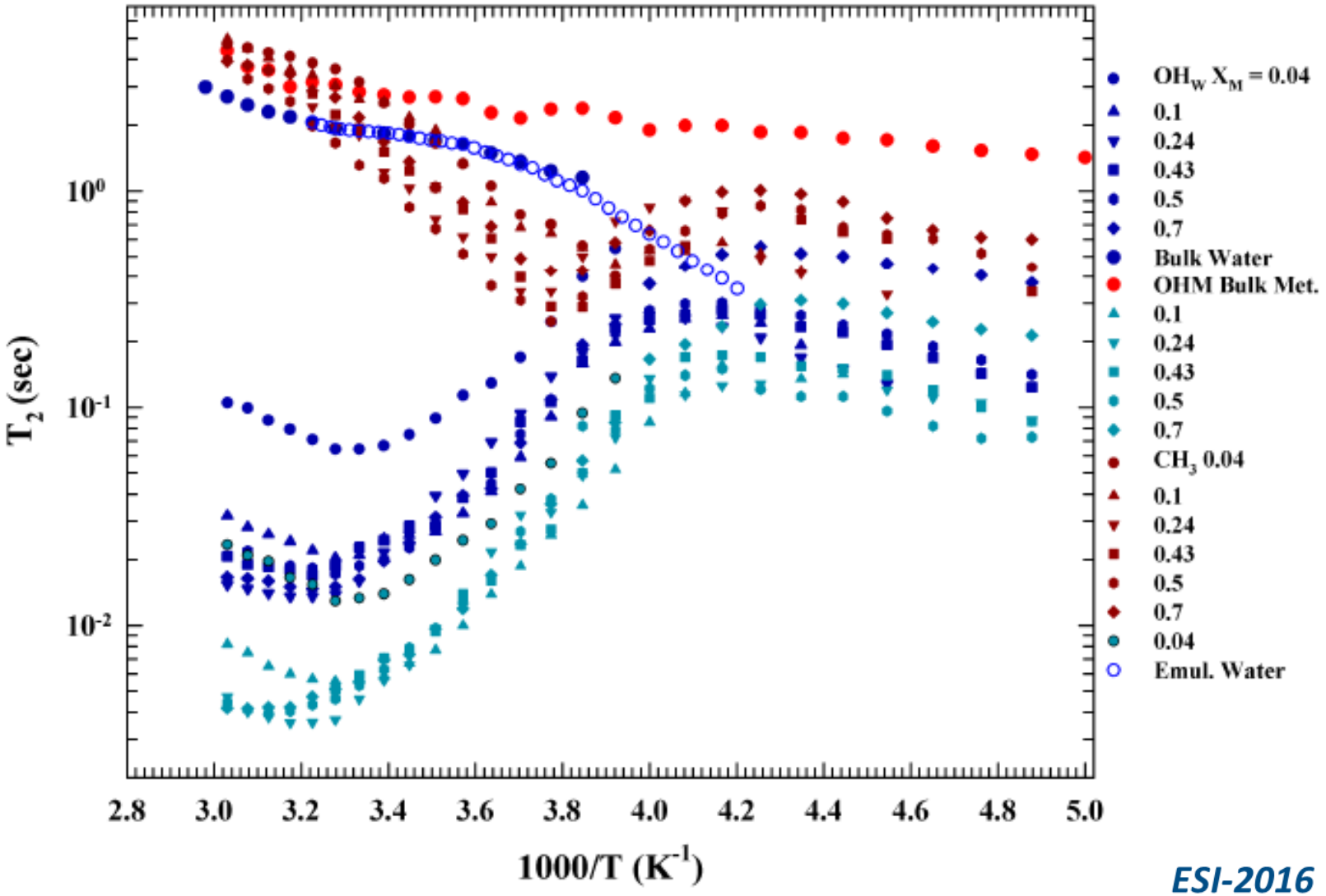

ESI-2016

All the evaluated BPP relaxation times, τ_c, for bulk water and methanol (top), the hidroxyl (middle) and the methyl groups (bottom).

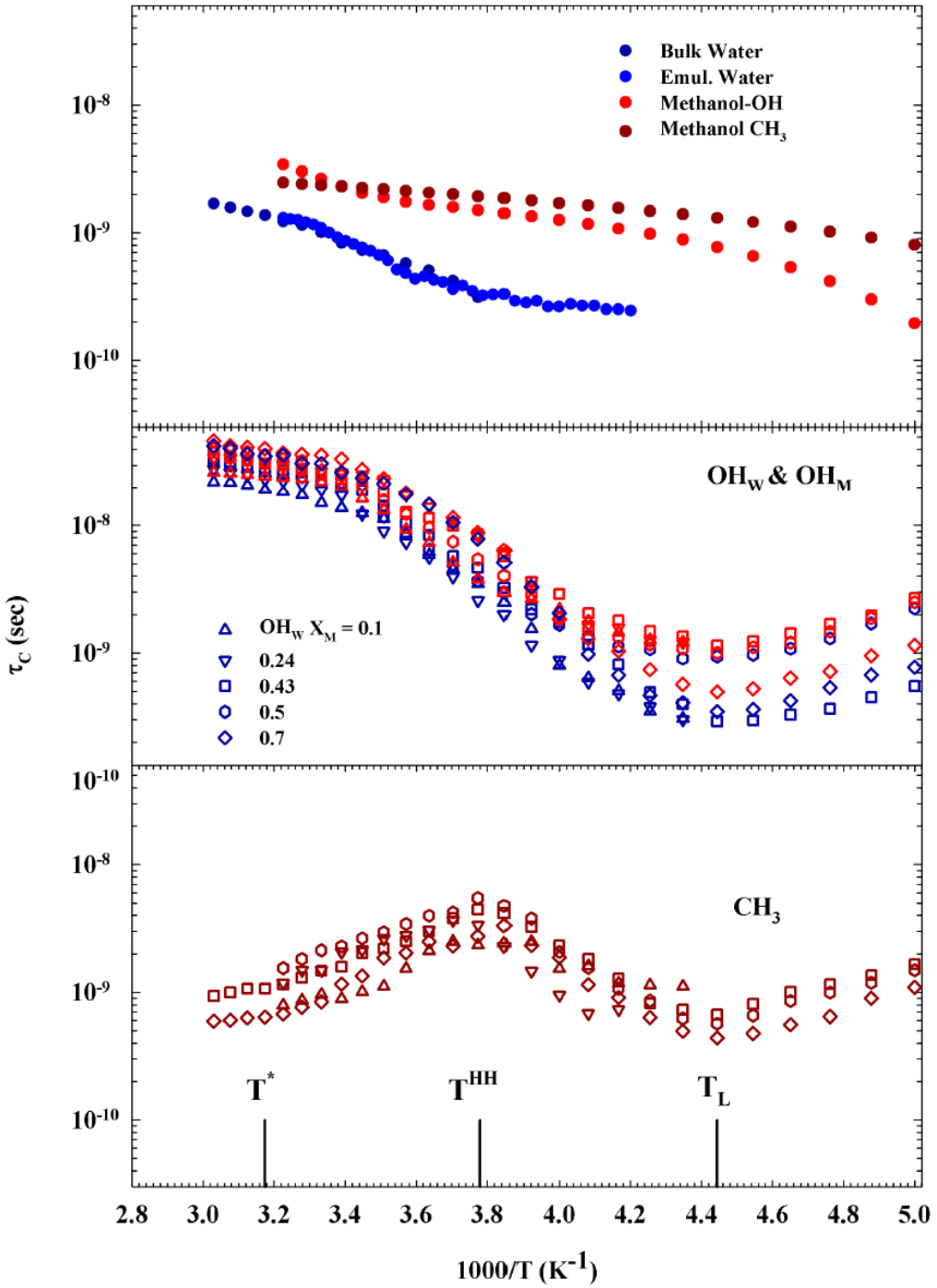

ESI-2016

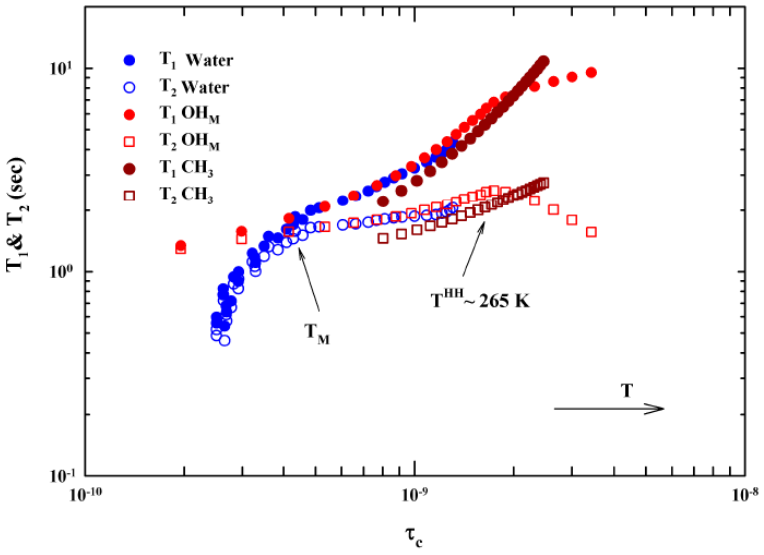

The BPP plots for bulk water and methanol and their solutions.

ESI-2016

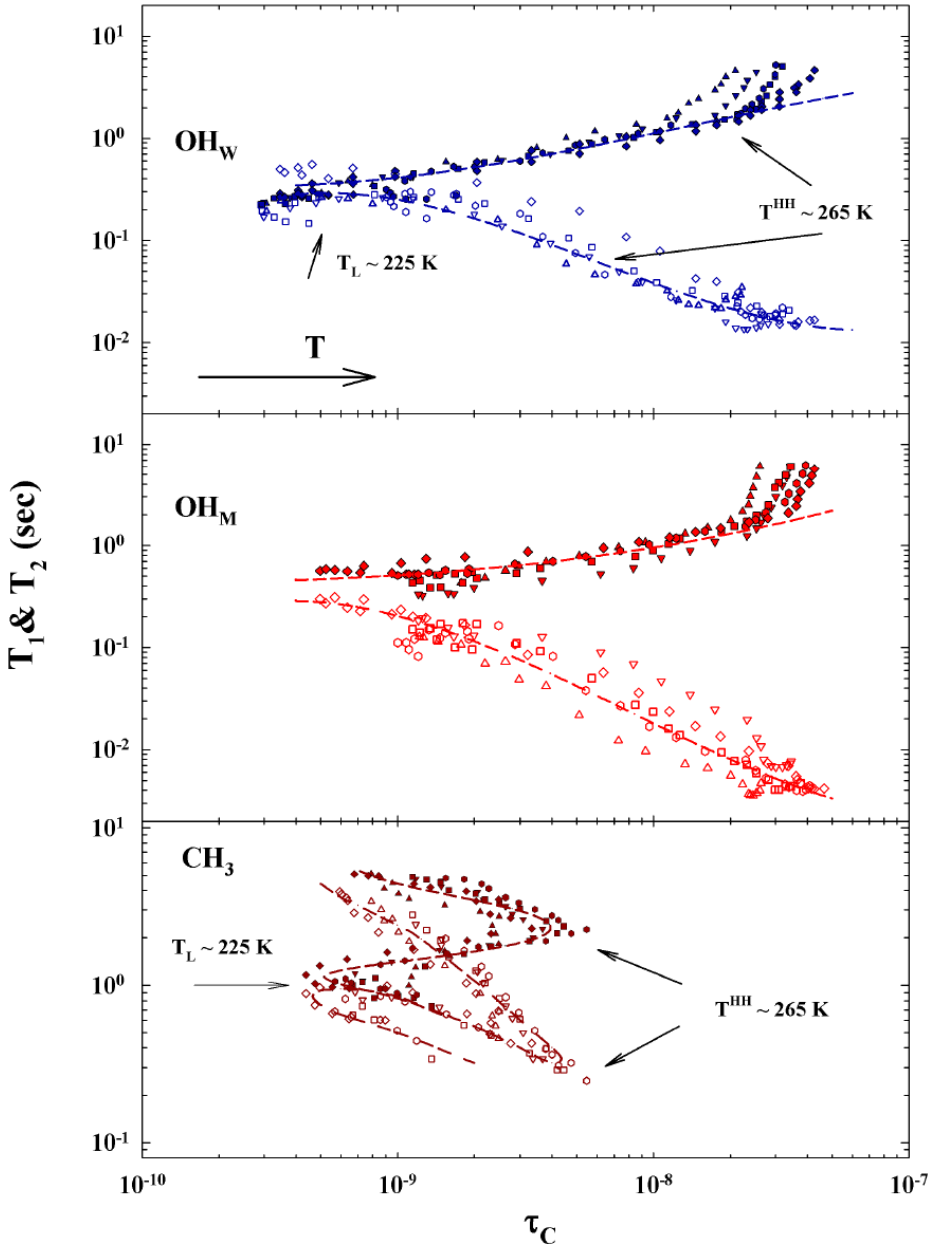

Arrhenius plot of the Kubo-Tomita-Hubbard relaxation times (T_1 inter and intra; and the rotational τ_θ) for the water and the studied solutions , hydroxyl groups.

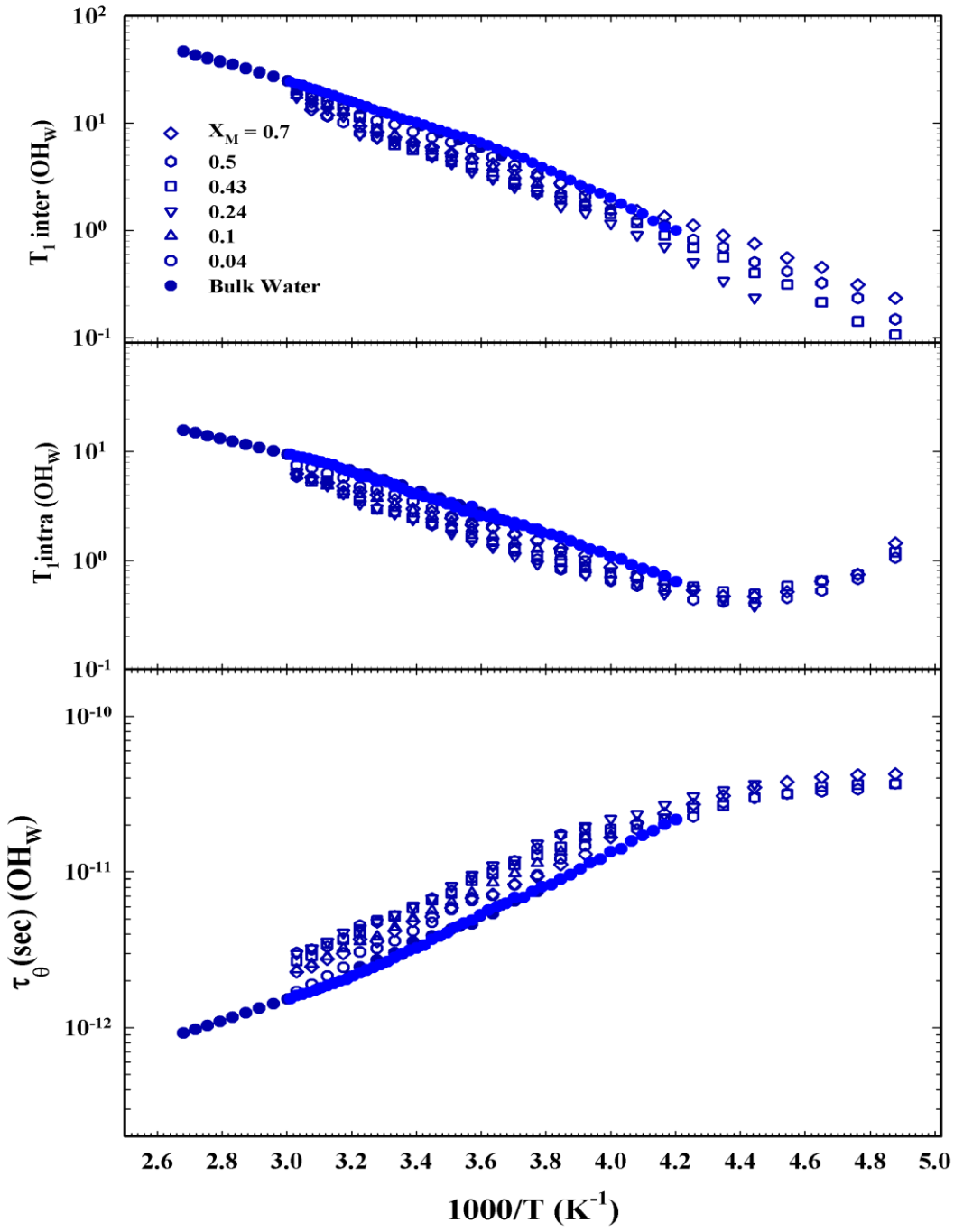

Arrhenius plot of the Kubo-Tomita-Hubbard relaxation times (T_1 inter and intra; and the rotational τ_θ) for the methanol and the solutions, hydroxyl groups.

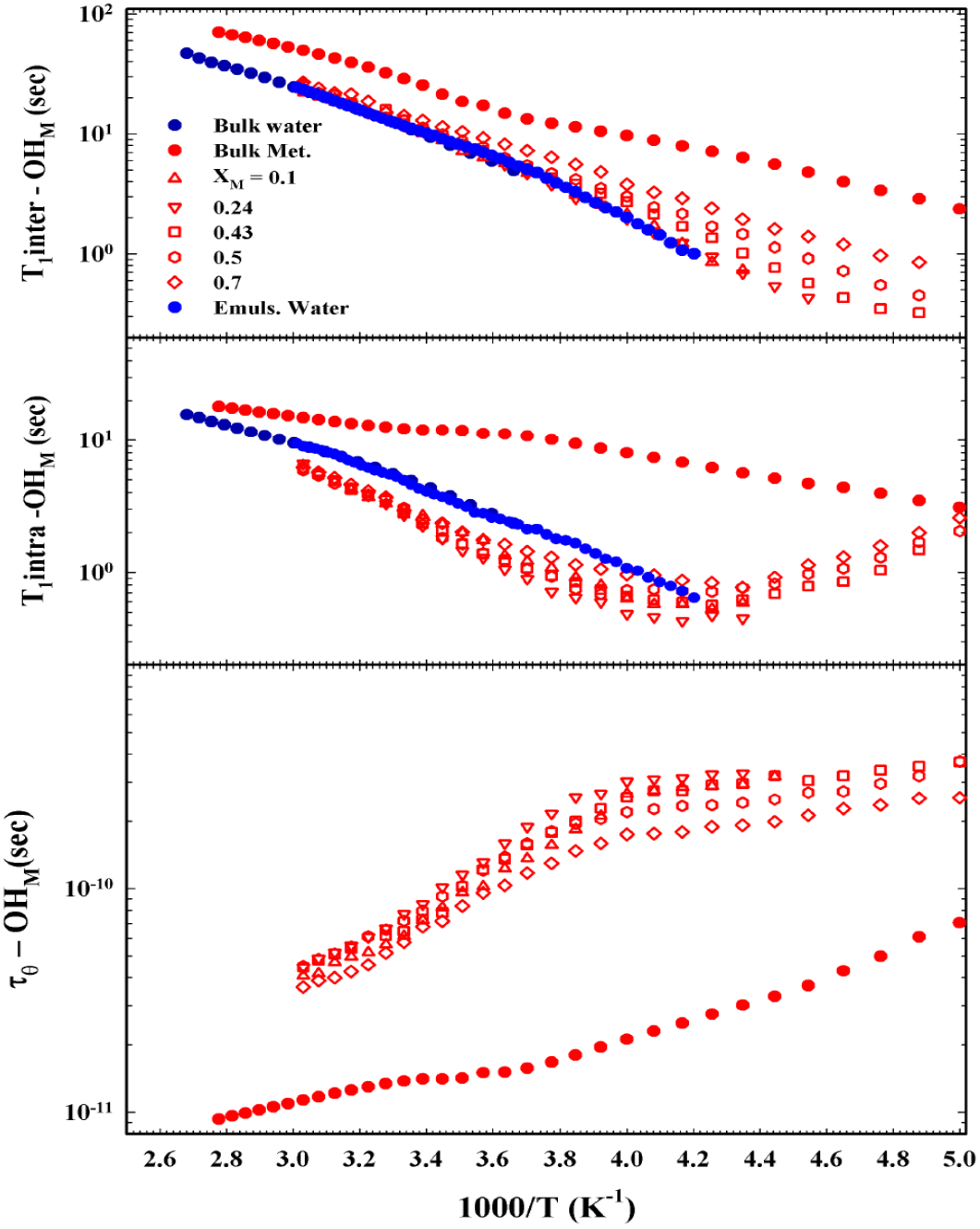

ESI-2016

Arrhenius plot of the Kubo-Tomita-Hubbard relaxation times (T_1 inter and intra; and the rotational τ_θ) for the methanol and solutions methyl groups.

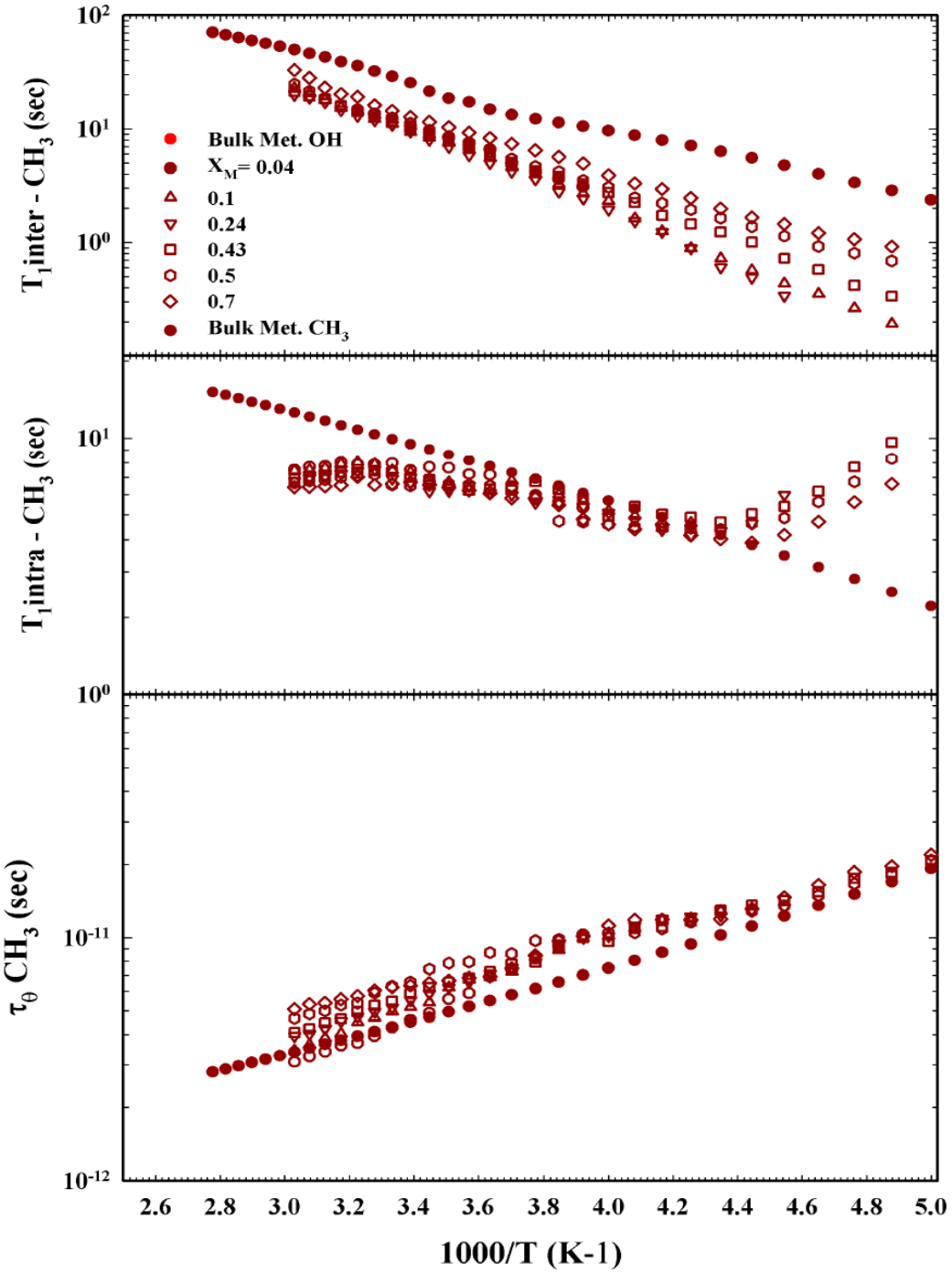

Comparative Arrhenius plots of the Kubo-Tomita-Hubbard relaxation times (T_1 intra; and the rotational τ_θ) for the hydroxyl and methyl groups.

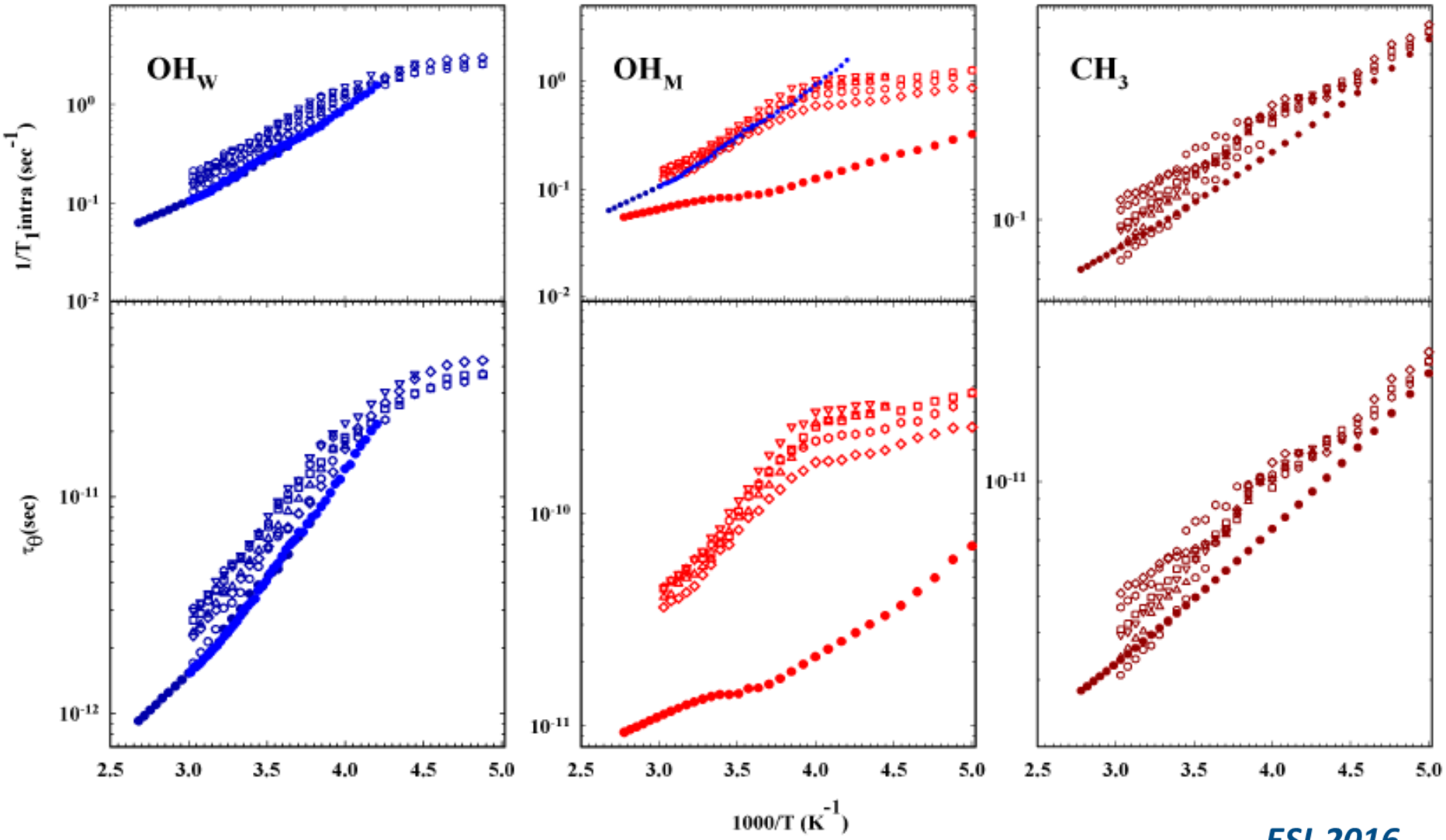

ESI-2016

ESI-2016

Arrhenius plot of the Kubo-Tomita-Hubbard rotational times (for the bulk water and methanol and the several solutions.

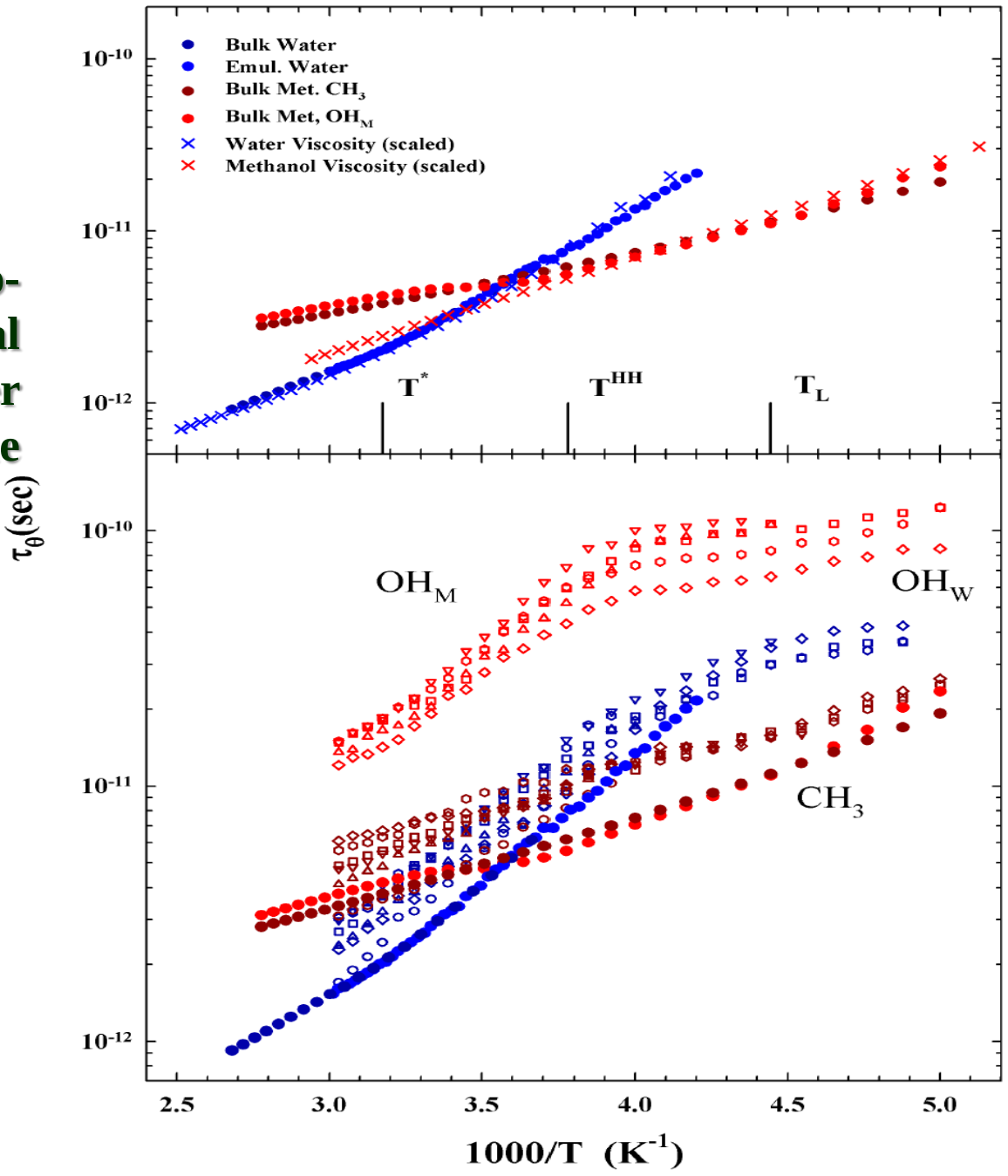

The spin-lattice relaxation time versus the corresponding τ_θ

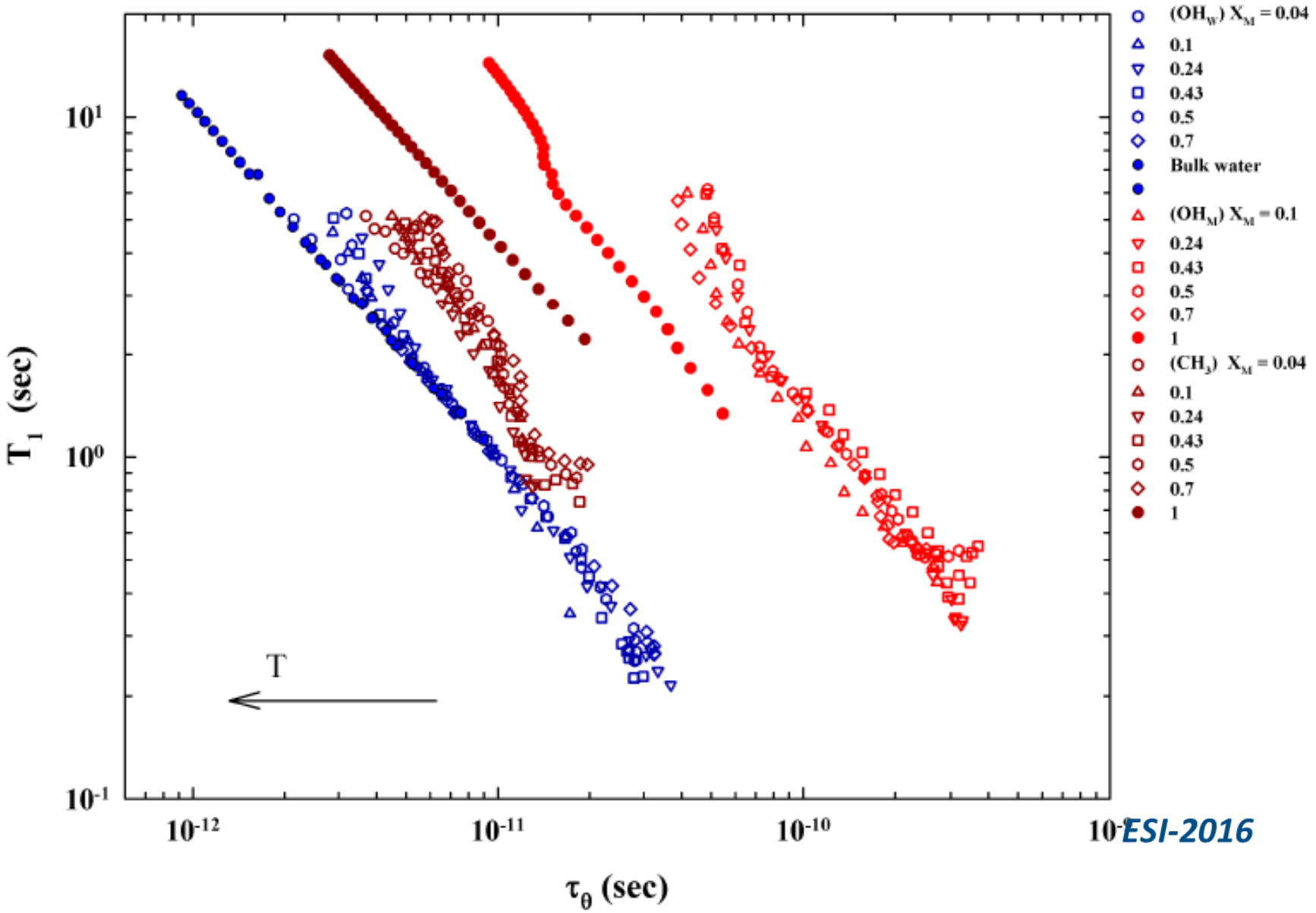

ESI-2016

The spin-spin relaxation time versus the corresponding τ_θ

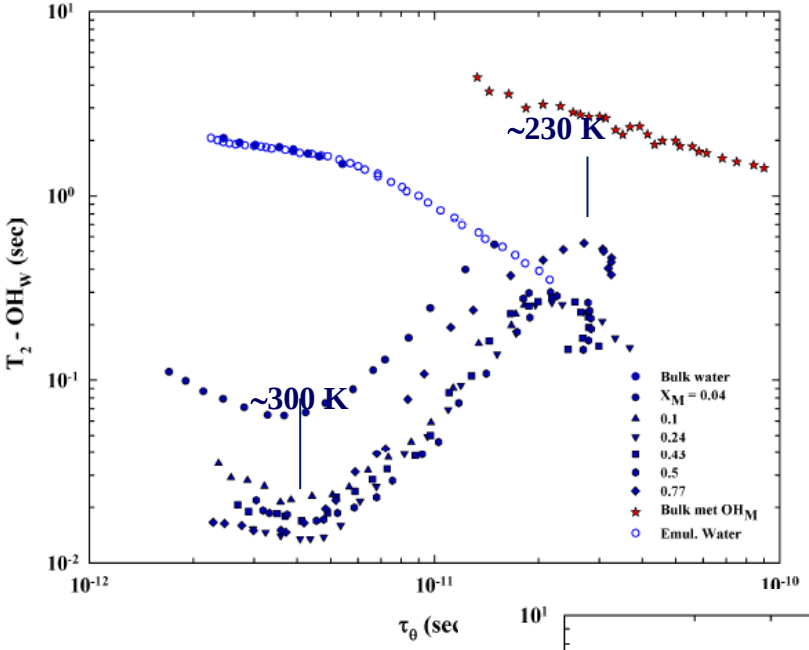

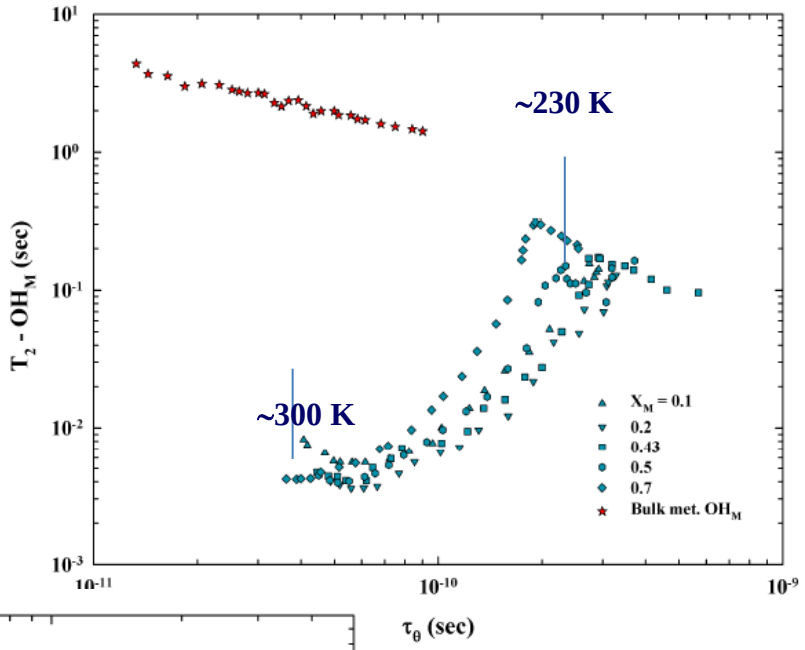

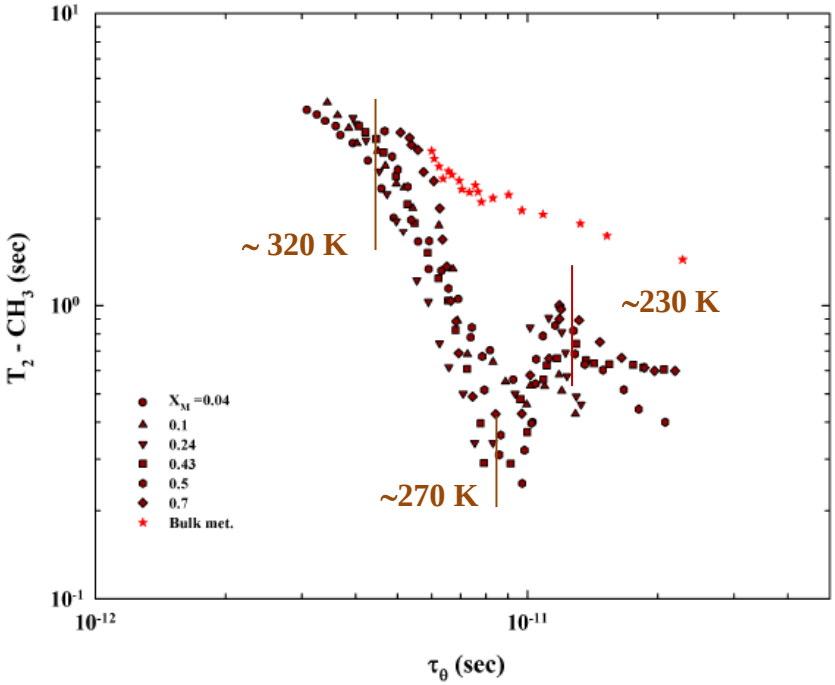

ESI-2016

CONCLUSIONS

- **The mutual properties of hydrophilicity and hydrophobicity can be studied in these water-alcohol solutions by using both the Bluembergen, Purcell and Pound (BPP) and Kubo, Tomita and Hubbard (KTH) approaches.**
- **The reported NMR results give evidence , especially from the thermal evolution of the CH_3 relaxation times, that the hydrophobicity becomes significant (and effective) for the solution properties inside the water stable liquid phase (T > 273 K).**
- **We have determined the reciprocal effects of the solvent on the solute and vice versa. Also evaluating the effect solutes have on the structure and energetics of the solvent.**

$$C(E_1, E_2, \emptyset) = \sqrt{8{E_1}^3 / M_N {L_0}^2}\, I(E_1) D(E_2) \left(\sum_M N_M \frac{\partial^2 \sigma_M}{\partial \Omega \partial E_2} \right) d\Omega \mathrm{d}$$